Int. J. Heat Mass Transfer. Vol. 8, pp. 1387–1414. Pergamon Press 1965. Printed in Great Britain

THE THERMAL CONDUCTIVITY OF LIQUID AND GASEOUS AMMONIA, AND ITS ANOMALOUS BEHAVIOUR IN THE VICINITY OF THE CRITICAL POINT

D. P. NEEDHAM and H. ZIEBLAND

Ministry of Aviation, Explosives Research and Development Establishment, Waltham Abbey, Essex

(*Received* 2 *November* 1964 *and in revised form* 12 *May* 1965)

Abstract—The thermal conductivity of liquid and gaseous ammonia has been determined between 20° and 177°C and at pressures from 1 to 500 atm using a vertical, co-axial cylinder apparatus.

Measurements in the vicinity of the critical point (p_c = 111·5 atm, t_c = 132·4°C) have been carried out with special care along the reduced isotherms, 1·016 and 1·061. An anomalous increase of thermal conductivity in this regime has been found, similar to that for carbon dioxide previously reported by two other observers. A tentative explanation of this phenomenon, based on transport of energy by clusters of molecules, is given.

Experimental results for the liquid-like fluid state, both below and above the critical temperature, have been correlated by a quadratic equation between density and thermal conductivity. With the aid of this equation, values have been computed for conditions outside those of this study, and the table containing the smoothed, experimentally verified figures at even increments of pressure and temperature has been complemented by computed values ranging up to 1000 atm and 480°K. Computed values are also presented in tabular form for the technically important temperature range from room temperature to the normal fusion point (195·5°K).

To provide a general survey, and for rapid interpolation, experimental results are presented also in the form of two diagrams, in which isobars and isotherms of the thermal conductivity are shown, using temperature and pressure, respectively, as the independent variables.

Low pressure, gas phase data of previous observers and those of this research have been reduced to 1 atm with the aid of pressure coefficients derived from this study. Using the relation for the thermal conductivity of polar gases, proposed by Mason and Monchick, the results of all sources have been satisfactorily correlated between 300° and 500°K.

The results of this work agree well with the few dense gas phase data reported by Keyes, and are in perfect agreement with tentative data along a short section of the saturation line given by Sellschopp in the only reference found on the thermal conductivity of liquid ammonia.

Considering all known causes of error, the accuracy of this study is estimated to be within ±1·5 per cent for the liquid and dense gas phases, and within ±2 per cent for the low-pressure gas phase and the near-critical region.

1. INTRODUCTION

AMMONIA has been used extensively in chemical industry as one of the basic materials, and it is an important working fluid in the refrigeration industry. In view of its physical and chemical properties, it has also been considered as a fuel and coolant for high energy, liquid propellant rocket engines.

Heat transfer to and from ammonia is an important process during its production and in its various applications, particularly in the field of rocket engineering. For the analysis and prediction of heat-transfer conditions, knowledge of the thermal conductivity of the working fluid is one of the essential prerequisites. In view of the special importance of ammonia and the diversity of its applications, such data are required over a wide range of temperature and pressure, including the critical point.

In contrast to the requirements, information on the thermal conductivity of gaseous ammonia at pressures in excess of 1 atm is scant, and information on the thermal conductivity of the liquid and solid phases is almost non-existent.

Several investigators have measured the thermal conductivity of gaseous ammonia at, or below, atmospheric pressure [1–6], but only Keyes [7] has given values between 50° and 250°C at pressures up to 9 atm.

For the liquid phase at 12 atm pressure, Kardos [8] suggested an average value for the temperature range −10° to +20°C. Sellschopp [9], who like Kardos had encountered difficulties with his apparatus, proposed tentative values between 30° and 100°C at the appropriate saturation pressure. No experimental studies at higher pressures of either the gas or liquid phase have been published yet, although work of this kind is in progress elsewhere [10]. A single value for solid ammonia at −104°C has been given by Eucken and Englert [11].

Theoretical studies of the thermal conductivity of ammonia have been made by Franck [12] and by Groenier and Thodos [13]. The former derived a semi-empirical relation between thermal conductivity, specific heat and specific volume for predicting conductivity in the gas phase up to pressures of 60 atm between −50° and 150°C, whereas the latter authors applied the principle of corresponding states to the few known experimental values to design a chart of reduced conductivity against reduced temperature with reduced pressure as a parameter.

Experimental determinations of the thermal conductivity of specific liquids of direct interest to modern technological developments (rocket engineering, atomic power engineering) have been carried out at the Explosives Research and Development Establishment over several years. In view of the probable importance of ammonia as a rocket fuel and coolant, and the undoubted practical interest in such data, the thermal conductivity of ammonia has been investigated over wide ranges of pressure and temperature in the vapour and liquid phases. Results for the liquid and liquid-like fluid state only, at saturation vapour pressures up to 200 atm, have been presented previously at the A.S.M.E. 2nd Symposium on Thermophysical Properties, Princeton, 1962 [14].

2. DESCRIPTION OF METHOD

A vertical, coaxial cylinder apparatus with guard rings was used for these measurements. In this method, heat is generated by an electric heater in an inner emitting cylinder and passed radially outwards through a narrow fluid-filled annulus to a surrounding receiving cylinder.

From the measured temperature difference between the emitting and receiving surfaces, the heat flow calculated from electrical data and the accurately known dimensions of the apparatus, the thermal conductivity is computed from the equation:

$$k = -Q \ln (r_2/r_1)/\{2\pi L (t_2 - t_1)\} \qquad (1)$$

where k is the thermal conductivity (cal/cm s degC),

Q, the heat flow (cal/s),
r_1, r_2, the radii of emitting and receiving cylinders, respectively (cm),
L, the length of the emitting cylinder (cm),

and t_1, t_2, the surface temperatures of the emitting and receiving cylinders, respectively (degC).

3. EXPERIMENTAL

3.1 *Conductivity cell and high pressure autoclave*

The conductivity cell and autoclave were essentially the same as those used by Ziebland and Burton [15]. The emitting, receiving, and guard cylinders used in these tests were made of a 99:1 silver–copper alloy (Johnson Matthey Ltd., London). The cell dimensions, from which the cell constant was calculated, were supplied by the makers, The Pitter Gauge and Precision Tool Co. Ltd., Woolwich. The annulus width was 0·0197 ± 0·00013 cm at 20°C.

The emitting cylinder and the two adjacent guard rings, separated by 1 mm thick mica spacers, were mounted on a close fitting, high tensile steel tube which contained the complex electric heating element. This tube, closed at one end, was joined by a loose flange connection to the autoclave lid. A three-armed support at the lower end of the tube supported the receiving cylinder which was mounted coaxially with respect to the emitting cylinder with the aid of mica strips secured by grub screws. Uniformity of the annulus width was checked by slip gauges. Immediately before the assembly of the cell, the emitting and receiving surfaces were highly polished. This, together with the low

emissivity of silver, serves to minimize heat transfer by radiation.

The four thermocouples which were used for measuring the required temperatures in the conductivity cell, were placed in pressure-tight sheaths of stainless steel so as to prevent direct contact with the fluid and thus eliminate electrical effects during the study of conducting substances, and also exclude the effect of pressure (strain) on the thermal e.m.f.s generated. These sheaths passed through the autoclave lid, to which they were sealed by soft aluminium washers, and entered close fitting holes drilled in the conductivity cell cylinders. The lengths of the sheaths were such that the thermocouple junctions were positioned at the centres of the emitting and of the receiving cylinders, and in the upper and lower guard rings, 3 mm from the interface with the emitting cylinder.

With this arrangement, the junctions were located beneath the respective surfaces whose temperatures were required for the evaluation of equation 1, and hence corrections proportional to the heat flux had to be applied to the measured temperatures. The corrections were small due to the short distance (3·5 mm) of the junctions from the respective surfaces, and the high conductivity of the silver alloy (see Section 3.5.3).

The cell was contained in a Monel autoclave, differing from that shown in [15] only in having a more massive lid and stronger retaining bolts to withstand a maximum operating pressure of 500 atm at 200°C.

The electric heater in the centre of the emitting cylinder consisted basically of three uniform, but electrically separately controlled, windings of constantan wire, 30 S.W.G. They were wound on a former made from six thin-walled glass tubes uniformly spaced round a stainless steel tube inserted for greater rigidity, and as support for the terminal connections. Current leads of 25 S.W.G. silver wire passed through the glass tubes and connected to the windings, while potential leads of 30 S.W.G. silver wire were connected to the 10 cm long central (emitter) winding. Several layers of glass fibre tape were wrapped round the assembly to strengthen it, and also to produce an approximately circular cross section of 9 mm external diameter. The heater passed through the autoclave lid into the closed tube supporting the conductivity cell, making a close fit with the tube. Contact between the test fluid and the heating element, a cause of failure in the experiments of earlier workers [8, 9], was prevented by this arrangement. The position of the centre 10 cm of the heater coincided with the length of the emitting cylinder, the positions of the other two windings with those of each guard ring. Independent control of the energy dissipation in the emitter section and the guard rings was obtained by varying the current flows by means of three sets of finely adjustable series resistances. Direct current was used as the energy source and was supplied by a large capacity Ni/Fe battery.

3.2 *The cylindrical thermostat*

The autoclave assembly (E) was suspended from the lid of the completely enclosed, cylindrical thermostat (D) as shown in Fig. 1. The heat-transfer fluid used (Thermex, I.C.I. Ltd.) is liquid in the range 12°–255°C at atmospheric pressure. This fluid has no toxic effects, but its penetrating smell is undesirable in a laboratory. Hence all connections passing from the autoclave through the thermostat were sealed by rubber O-rings and an open, water-cooled reflux condenser was located on top of the thermostat lid to prevent the escape of fumes into the atmosphere.

The thermostat fluid was heated electrically, and was circulated round concentric baffles by a submerged centrifugal pump. A coil, through which mains water could be circulated, acted as a heat sink and was provided in order to carry out measurements near to ambient temperature. In most cases, temperature control was by a resistance thermometer controller (Sunvic Controls Ltd., Type R.T.2) giving stability to 0·05 degC, but for measurements below 30°C, an electronic thermostat (Fielden Electronics Ltd.) was used. In both controllers, platinum resistance thermometers were used as temperature sensing devices. These were placed in a sealed tube close to the heating coils. The whole apparatus was suspended from a framework by chains and was thermally insulated.

3.3 *The pressurizing system*

For experimental purposes, it was essential to

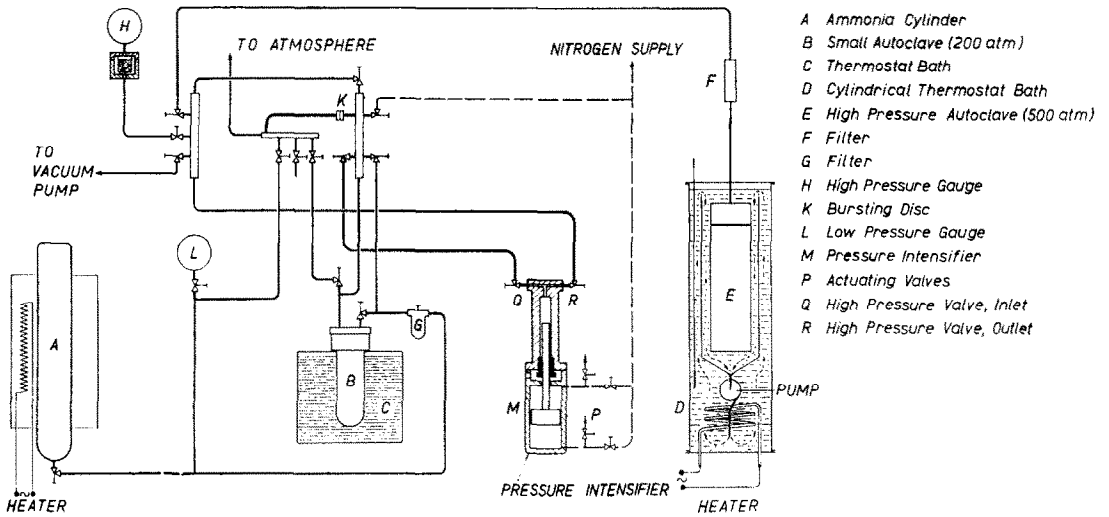

FIG. 1. Schematic lay-out of experimental apparatus.

adjust and maintain accurately the pressure of the test fluid at any chosen pressure level up to 500 atm. The use of conventional devices, such as hydraulic rams employing lubricated pistons, or a mercury piston, had to be ruled out because of (a) the solubility of lubricants in high-pressure liquid ammonia and subsequent contamination of the sample and the surfaces of the conductivity cell, (b) the possibility of ammonia at high pressure forming compounds with mercury which could detonate on depressurization, or during the removal of contaminated ammonia [16].

A thermal compressor was used in this investigation for pressures up to 200 atm (see Fig. 1). It consisted of a small autoclave (B) of about 500 cm^3 capacity immersed in a temperature-controlled liquid bath (C). With the autoclave, conductivity cell, and pipework filled with liquid ammonia, and the supply cylinder closed off, the appropriate pressure rise was obtained from the thermal expansion of the liquid by heating the thermostat bath to a suitable temperature. The temperature stability of the bath was sufficient to maintain the pressure to within ± 1 atm of a chosen level for several hours.

The maximum operating pressure of the above device was limited by the mechanical strength of the components, largely that of autoclave (B), and the safe operating temperature of the thermostatic bath.

To extend the measurements to 500 atm, a pressure intensifier (M) was constructed and connected to the existing arrangement in such a manner that the two compression devices could be used in parallel but not simultaneously.

The pressure intensifier, of which details of construction and main dimensions are shown in Fig. 2, consists of two in-line cylinders with cross-sectional areas in the ratio 22:1. In the larger cylinder, a double-acting working piston is actuated by compressed nitrogen gas which is admitted and released through a manually operated valve system (P). The compressor cylinder contains a plunger directly connected by a rod to the actuating piston and is sealed to the atmosphere by a chevron-type packing fabricated in Teflon. The choice of a suitable type of packing ring and material presented some difficulty as no lubricant could be allowed to come into contact with the test fluid. The non-lubricated, dry, Teflon packing shown in Fig. 2 proved reliable for the required pressure of 500 atm. The actuating piston and the connecting rod were sealed in the larger cylinder by conventional, lubricated O-rings.

The operation of this device is almost self-explanatory from Fig. 2. With the plunger in the retracted position, the compressor cylinder was

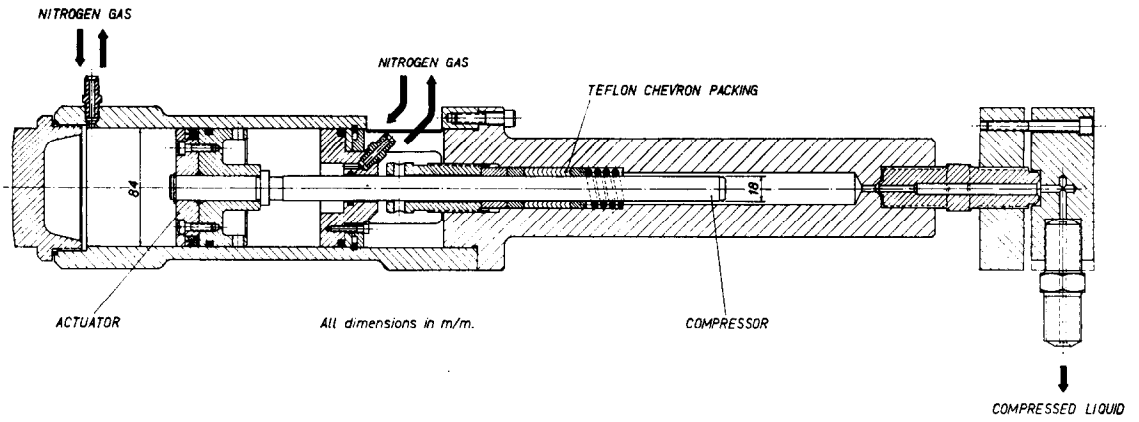

FIG. 2. Pneumatically operated pressure intensifier.

evacuated and then filled with liquid ammonia through the high pressure valve Q (Fig. 1). After closing valve Q and opening the companion valve R, nitrogen at 50–60 atm pressure was admitted beneath the driving piston, causing the plunger to move upwards and thus compress the liquid ammonia in the apparatus. By closing valve R, the pressure in the system could be retained during measurements. If required, the compressor cylinder could now be recharged with liquid for a further cycle of operation.

3.4 *Temperature measurement. Construction and calibration of thermocouples*

All temperatures were measured with copper–constantan thermocouples using an ice bath to provide a common reference temperature. The e.m.f.s generated were measured with a Diesselhorst potentiometer having a least count of 0·1 μV, which allowed the detection of temperature changes of approximately 0·002 degC. The couples were made of multistranded wires to minimize the effects of inhomogenities. The hot junctions were silver soldered into short copper cylinders which were sealed into, but electrically insulated from, the ends of 85 cm long, thin-walled, stainless steel tubes by means of a thermo-setting "Araldite" resin. Electrical insulation of the thermocouple leads within the tubes was provided by twin-bore alumina tubing. At the upper end of the stainless steel tube, the wires were joined to copper and constantan terminals, respectively. After prolonged heating of the assembly to over 100°C to remove absorbed moisture from the alumina tubing, the terminal end of the thermocouple was sealed with Araldite.

The cold junctions were also made from multistranded wires, but joined by soft soldering, and insulated by plastic sleeving. Each assembly was sealed with wax into a closed glass tube to prevent condensation of moisture. The glass tubes were inserted into a copper block which was immersed in the ice bath.

The constantan wires of the cold junctions connected as single lengths of wire to the hot junction constantan terminals; the copper wires from the cold junctions and the extension leads from the hot junctions connected to metal terminal boxes which formed isothermal enclosures, and from which copper multicored cables joined the couples to the potentiometer.

To calibrate the thermocouples, they were placed in a copper block of the same size and shape as the autoclave with holes drilled to depths corresponding to those in the autoclave. The block was immersed in the thermostatic bath. A central hole in the block accommodated a N.P.L.-calibrated platinum resistance thermometer which provided the reference standard; the variation of its resistance with temperature was determined by a precision Smith's Differential Bridge (Cambridge Instrument Co.).

Seven couples were calibrated, four for use at any one time, with a spare couple for each depth of immersion in the conductivity cell. The couples were calibrated at narrow intervals of

temperature over the range 0°–180°C to give a series of e.m.f. values, E, as a function of the temperature, t (°C). By least-square analysis of these values, the E versus t relationship for each couple was determined, quadratic equations being found adequate to define this relationship within the above temperature range. From the equations of the form $E = at + bt^2$, calibration tables for each couple were calculated for temperature intervals of 1 degC. Within these intervals, linear interpolation was employed.

Although the couples were constructed from multistranded wires, small differences of not more than 1 μV (equivalent to approximately 0·02 degC) were observed for the same temperature between individual couples. The four most nearly identical couples were selected for use in the conductivity measurements, the two closest couples (differing by less than 0·3 μV) being taken for use in the emitting and receiving cylinders. As the couples had been calibrated in the positions which they were to occupy in the conductivity cell, effects due to variable depth of immersion were eliminated.

The reliability of thermal conductivity measurements depends to a great extent on the precise determination of small temperature differences between various parts of the conductivity cell. Whilst a random change in the absolute calibration of 1 μV at a level of, say, 100°C would result in an absolute error of about one part in 5000, the resultant error in the important temperature difference across the fluid annulus, which was generally about 1 degC, would be one part in 50, i.e. 2 per cent. Similar, though perhaps not so stringent requirements apply to the couples located in the guard rings, whose temperature differences relative to the thermocouple located in the centre of the emitting cylinder, are proportional to the amount of axial heat loss or gain.

To ensure freedom from small individual random changes of the various thermocouples, inter-calibrations were carried out at frequent intervals of time with the couples *in situ*. At each new level of temperature, the cell heater was switched off and the cell and autoclave allowed to reach thermal equilibrium. The thermal e.m.f.s generated by all couples were measured and their differences compared with those obtained from the calibration charts at the corresponding temperature levels. No significant changes, permanent or temporary, with respect to the emitter thermocouple were found for any of the other thermocouples, during the course of this investigation.

3.5 *Evaluation of the thermal conductivity and a discussion of the correction terms*

3.5.1 *The cell constant.* The equation for evaluating the thermal conductivity, equation 1, contains the term $\ln (r_2/r_1)/2\pi L$, which is solely dependent on the dimensions of the conductivity cell, and is a constant at any one temperature. It is commonly referred to as the geometric cell constant. Its value was calculated for various temperatures within the temperature range of these experiments from the measured cell dimensions at 20°C and the coefficient of thermal expansion of silver [17]. In view of the very low compressibility of metals, pressures of the magnitude employed in these tests had an insignificant effect on the cell dimensions.

3.5.2 *Heat energy dissipation.* The energy, Q, dissipated in the cell was measured electrically from the current flowing through the central 10 cm of the heater, which coincided with the length of the emitting cylinder, and the potential difference across this length.

The current was evaluated from the measured potential difference across a series standard resistance of 0·01 Ω, the potential difference being obtained by the use of a potential divider with the ratio 10^4:1 in parallel with the heater winding. Both these e.m.f.s were measured with the same Diesselhorst Potentiometer employed for measuring the thermal e.m.f.s of the thermocouples.

To convert electrical units into thermal energy units, the conversion factor of 4·1853 J/cal was used. A multiplier derived from this factor and the electrical resistances of the measuring circuit related energy dissipation, Q, to the measurements of potential difference and current.

3.5.3 *Mean temperature and temperature difference.* The temperatures of the emitting and receiving cylinders were evaluated separately from the e.m.f.s of the two thermocouples located in the central plane of these cylinders. The temperature of a measurement was taken as the

mean temperature of these two values, while their difference gave the observed temperature difference. Since the junctions of these thermocouples were not on the surfaces of the cylinders, but at known distances beneath them, a correction to the observed temperature difference allowed for the temperature drop through the metal layer between the thermojunction and the respective surface. The correction was evaluated for each individual determination from the heat flow, Q, and a factorial term dependent on the cell geometry and the thermal conductivity of the material of construction [17]. In all cases, the value of this correction did not exceed 4 per cent of the observed temperature difference, and, for most measurements, it was considerably less than 4 per cent.

3.5.4 *Axial heat flow.* Axial heat losses or gains from the ends of the emitting cylinder were minimized by careful adjustment of the guard ring heater currents to ensure that the temperature differences between the emitting cylinder and the guard rings were as small as possible. The temperature difference permitted was never more than the reproducible limit of accuracy of the guard ring thermocouples, i.e. ± 1 μV, corresponding to a temperature difference of 0·02 degC. A temperature difference of that magnitude would cause an error of less than $\pm 0{\cdot}2$ per cent in the least favourable case of axial heat flow to or from both guard rings in the same direction. The improvement in the reproducibility of the thermocouples compared with those used in the previous study [15], has been achieved by more refined construction and better calibration.

3.5.5. *Radiation correction.* The use of silver for the construction of the cell, and the highly polished finish of the emitting and receiving surfaces, ensured that radiative heat exchange across the annulus would be small (Section 3.1). Completely ignoring the existance of absorption bands of ammonia in the infra-red region, which would tend to reduce such an energy exchange, an estimate of the radiative heat flux was made from measurements of the heat transfer across the annulus of the cell with the autoclave evacuated to 0·02 mmHg. Application of this correction to actual conductivity determinations showed that the computed radiative heat flux, in the most unfavourable operating conditions of low fluid pressure and high temperature, was approximately 0·5 per cent of the total heat flux. In all other determinations, the effect was considerably less and hence negligible compared with the random experimental scatter.

3.5.6 *Convection effects.* In order to avoid errors due to the onset of thermal convection, all measurements were made with the smallest temperature difference across the annulus compatible with the precision of the thermocouples. Where the physical data were known or could be estimated with reasonable precision, convection was considered absent if the product of the Grashof and Prandtl numbers was below the critical limit of 800. The absence of convection at other doubtful points was checked by determining the thermal conductivity at various heat inputs at identical values of pressure and temperature. For almost all conditions, these check values were identical within the accuracy limits.

Certain values, however, at conditions slightly above the critical point, were shown to be affected by convection, despite the use of small energy dissipations. These values were obtained at a temperature of 139°C and at pressures between 124 and 129 atm, and here a reduction of the heat dissipation Q, and consequent reduction of the temperature difference Δt across the annulus, caused a diminution in the magnitude of the thermal conductivity. To obtain convection-free values at each combination of temperature and pressure, the magnitude of Δt was progressively diminished until further reduction caused no change in the value of the thermal conductivity, within the limits of accuracy. These thermal conductivities were then considered to be free from convective effects. Typical examples of the variation of thermal conductivity with diminishing Δt are shown in Fig. 3.

3.5.7 *Heat losses in heater leads.* Measurements of the thermal conductivity of ammonia in the vapour phase were made for several isotherms over the pressure range from a few atmospheres to near the saturation vapour pressure for the given temperature. Due to the relatively low thermal conductivity in this region, only very small heater currents could be used.

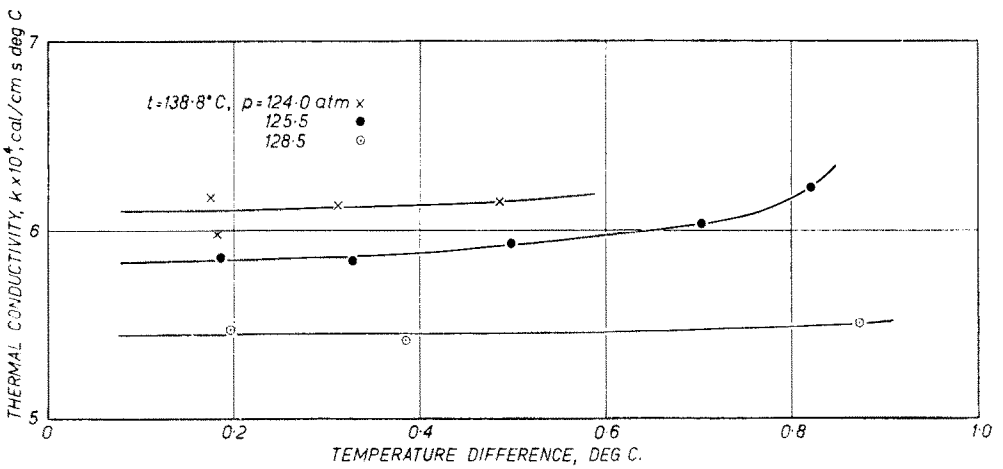

FIG. 3. Some typical examples showing the experimental determination of convection-free values (k constant) by progressive diminution of Δt.

The values obtained were found to be consistently higher than those of several previous authors [1–6]. Careful consideration of possible errors suggested that a small axial heat loss was occurring which had not been allowed for in the corrections to the radial heat flow (Section 3.5.2). The loss would be of the order of a few hundredths of a calorie per second and hence would be significant only in those measurements where small heat dissipations were used.

As a result of a general examination of possible paths of non-radial heat flow, attention was focused on the heating element itself, and it was realized that a small amount of heat could be lost axially along the two potential leads made of silver which were attached to the ends of the centre section of the heater winding. Although these wires are in a near-isothermal region at, and near, their point of attachment, they pass through the autoclave lid where they must lose heat to the thermostat fluid, which is at a temperature several degrees below that of the heater surface.

Analysis of the heat flow along a wire with radial losses to a surrounding medium at constant temperature allowed the heat loss from the two wires to be estimated, using calculated values for the temperature difference between the heater surface and the thermostat bath. The calculated heat loss at ambient conditions was in close agreement with that estimated from the difference between the results of this study and published values of the thermal conductivity of gaseous ammonia.

The correction for the axial heat loss along the potential leads was applied to all experimental values, its magnitude as a percentage of the total energy dissipated being a function of the heat flux itself.

In the liquid phase, and at the higher pressures at supercritical temperatures, where radial heat fluxes are relatively large, the correction was insignificant in comparison with experimental scatter. Smaller heat fluxes are necessary for determinations in the vapour phase, and at slightly supercritical conditions, and here, the correction varied from 0·9 to 4·0 per cent. Values in Table 1 corresponding to these latter conditions have been corrected for this heat loss.

3.6 *Purity of the liquid ammonia*

The substance used in these tests was anhydrous ammonia of not less than 99·98 per cent purity. The suppliers, I.C.I. Ltd., state that typical analyses show 50 to 150 parts per million impurity, consisting mainly of water, the remainder being oil and carbon dioxide.

No independent analyses were carried out. However, during the course of this investigation which extended over a period of about 21 months, the conductivity cell was emptied and charged with new fluid samples several times, these

samples being taken from three different cylinders. No noticeable difference was detected between the values pertaining to the samples from different cylinders, showing that the fluid was of consistent purity.

3.7 *Experimental procedure*

3.7.1 *The filling of the apparatus.* Liquid anhydrous ammonia was contained in the steel cylinder (A) from which it was drawn by using the cylinder in the inverted position. In order to maintain the stated purity of the substance, all air and traces of moisture had to be removed from the apparatus before any part of it was filled. This was achieved by prolonged evacuation of the system with a rotary vacuum pump, during which time all parts were heated to about 70°C to remove occluded moisture. The apparatus was heated by its own thermostat baths, the pipe-work by wound-on electrothermal tapes and by hot-air blowers as applicable. Evacuation continued as the apparatus cooled to room temperature.

Liquid ammonia was then transferred to the conductivity cell and other fluid-filled parts of the apparatus by heating the supply cylinder (A) to produce a cylinder pressure, shown on gauge (L), a few atmospheres above the saturation vapour pressure at room temperature. By opening appropriate valves, ammonia was admitted to the required sections of the apparatus where it condensed and remained in the liquid phase because of the excess pressure in the supply cylinder. Filters (F) and (G), in the high and low pressure lines respectively, prevented foreign matter from being carried into the autoclave. The working pressure in the autoclave was shown by an oil-filled gauge (H) which was separated from the high pressure fluid by a pressure-transmitting bellows. Several gauges were used to cover the pressure range with suitable accuracy and, in each case, the gauge and pressure transmitter were calibrated as a unit by means of a dead-load tester. A bursting disk (K) with a rupturing pressure of 240 atm was connected to the vent manifold and protected the low and medium pressure sections of the apparatus against inadventent pressure rise due to overheating of autoclave (B) or to a leak back from the pressure intensifier.

Some difficulty was experienced with leaking valves at the highest pressures. A modification was designed to convert a commercial, high-pressure, control valve with tapered spindle into a stop valve, in which a steel ball formed the sealing element. As there might be a wider application, this is shown in detail in Fig. 4.

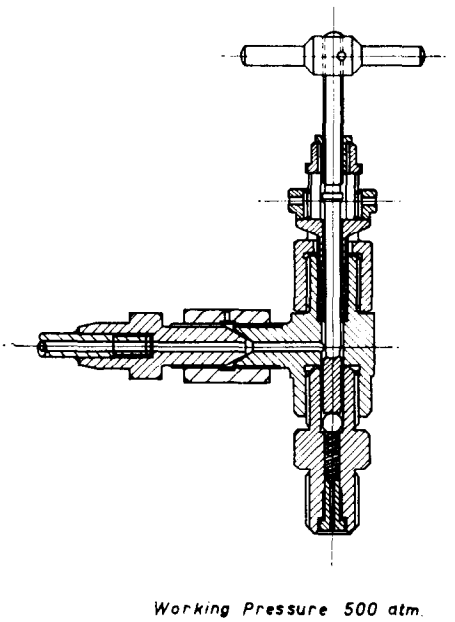

FIG. 4. High pressure stop-valve.

Sealing pressure on the ball was provided by a short spindle acting through a plunger of triangular cross-section. A light spring served to lift the ball off its seat when the valve was opened. The gland packing was made of Teflon. Such valves were tested by hydraulic pressure to 600 atm, and proved completely satisfactory in service with ammonia at pressures up to 500 atm.

3.7.2 *Determination of isotherms.* For experimental convenience, the individual thermal conductivity measurements were made at selected constant temperature levels, the pressure being varied as required (Section 3.3).

The determination of isotherms had advantages in speed of operation. The temperature of the cylindrical thermostat bath (D), which could be maintained at a set value for several days, determined roughly the temperature level in the

cell. The actual mean temperature of a measurement and the magnitude of the temperature difference across the annulus were determined by the heat dissipation of the electric heater. In the liquid, and liquid-like fluid states the effect of pressure on thermal conductivity was relatively small and a change in the pressure level caused only a small change in the mean temperature, which could be compensated for by a small adjustment of the energy dissipation in the heater. In the vapour phase, however, and in the region of rapid change of conductivity with pressure near the critical point, adjustments to the temperature of the thermostat bath itself were necessary to maintain a chosen mean temperature.

In general, all points on any one isotherm were obtained at mean temperatures within $\pm 0{\cdot}3$ degC of the nominal value. Consideration of the temperature coefficient of the thermal conductivity at constant pressure, calculated from several isotherms, showed that the errors produced by temperature variations of this amount were negligible. In the case of the 20·5°C isotherm, where control of the bath temperature was difficult, some values were measured at temperatures differing by as much as 0·6 degC from the mean. Corrections were applied to such values, the maximum correction being less than 0·4 per cent. At any selected value of pressure and temperature, at least three determinations of thermal conductivity were made over a period of 1–2 h and the arithmetic mean of the individual determinations taken as the most probable value. The temperature variation during any three such measurements was less than $\pm 0{\cdot}1$ degC.

The intervals of pressure selected along any isotherm were dependent on the appropriate isothermal pressure coefficient of the thermal conductivity. In regions of rapid change, measurements were made at closer intervals than were considered necessary in areas where the pressure effect was small.

In the case of two supercritical isotherms, viz. 139° and 157°C, measurements were made at pressure intervals as small as 1 atm in order to ascertain the presence of anomalous effects reported to occur at conditions of state corresponding to a density value equal to that of the critical density [25]. These conditions were reached at 131 atm for 139°C, and at 162 atm for 157°C; large numbers of determinations were made at close intervals of pressure over ranges of about 40 atm above and below these pressures.

4. EXPERIMENTAL RESULTS

4.1 *Presentation*

Table 1 contains the 115 measured values of

Table 1. *Thermal conductivity of ammonia. Experimental values*

Nominal temperature (°C)	Temperature of measurement (°C)	Pressure (atm)	Density (g/cm³)	Density (Amagat)	Thermal conductivity $k \times 10^4$ (cal/cm s degC)
20·5	20·625	1·2			0·582
	20·502	3·5			0·607
	20·849	6·2			0·644
	20·480	13·8	0·609	789·5	11·510
	20·381	94·3	0·617	800·0	11·668
	20·505	121·5	0·620	803·8	12·240
	20·498	142	0·621	805·1	11·908
	20·517	182	0·624	809·0	12·537
	20·438	200	0·625	810·2	12·077
	20·5	295	0·632	819·3	13·03
	20·5	466	0·643	833·6	13·28
59·3	59·396	44·5	0·552	715·6	9·788
	59·326	92	0·560	726·0	9·937
	59·402	107	0·563	729·9	10·218
	59·264	120·6	0·564	731·2	10·085

Table 1—continued

Nominal temperature (°C)	Temperature of measurement (°C)	Pressure (atm)	Density (g/cm³)	Density (Amagat)	Thermal conductivity $k \times 10^4$ (cal/cm s degC)
59·3	59·364	160	0·569	737·6	10·440
	59·385	162	0·570	738·9	10·245
	59·345	187	0·572	741·5	10·580
	59·296	196	0·574	744·1	10·357
	59·265	295	0·584	757·1	10·969
	59·399	468	0·600	777·8	11·524
90·6	90·604	2·8			0·786
	90·580	13·0			0·854
	90·649	29·3			0·965
	90·686	43·9			1·129
	90·597	60	0·484	627·4	7·826
	90·546	72·6	0·488	632·6	8·144
	90·569	93	0·495	641·7	8·087
	90·558	101·5	0·497	644·3	8·223
	90·544	144	0·508	658·6	8·464
	90·562	145·5	0·508	658·6	8·661
	90·616	171	0·514	666·3	8·737
	90·585	176	0·514	666·3	8·832
	90·545	209	0·521	675·4	8·880
	90·628	287	0·534	692·3	9·360
	90·604	461·5	0·558	723·4	10·072
119·1	119·065	2·8			0·865
	119·078	11·4			0·901
	119·183	32·8			1·026
	119·081	52·8			1·227
	119·129	71·2			1·523
	119·146	81·2			1·891
	119·048	99·5	0·395	512·1	6·345
	119·086	116	0·413	535·4	6·677
	119·103	134	0·428	554·8	6·802
	119·104	166·5	0·447	579·5	7·067
	119·151	166·5	0·447	579·5	7·159
	119·090	201	0·460	596·3	7·342
	119·114	282·5	0·483	626·2	7·994
	119·123	468	0·519	672·8	8·850
126·8	126·797	113	0·367	575·8	5·908
	126·795	143	0·404	523·7	6·295
	126·809	167	0·423	548·4	6·551
	126·820	200·5	0·442	573·0	6·841
138·8	138·805	100	0·088	114·1	1·977
	138·796	119	0·158	204·8	3·366
	138·743	120·5	0·166	215·2	3·978
	138·819	123	0·184	238·5	5·39
	138·818	124	0·193	250·2	6·10
	138·793	125·5	0·206	267·1	5·83
	138·830	128·5	0·231	299·5	5·44
	138·848	131	0·249	322·8	5·417
	138·782	135	0·275	356·5	5·413
	138·841	135·5	0·278	360·4	5·488

Table 1—continued

Nominal temperature (°C)	Temperature of measurement (°C)	Pressure (atm)	Density (g/cm³)	Density (Amagat)	Thermal conductivity $k \times 10^4$ (cal/cm s degC)
138·8	138·791	136	0·281	364·3	5·326
	138·868	142	0·310	401·9	5·578
	138·753	149	0·336	435·6	5·603
	138·750	181	0·391	506·9	6·101
	138·822	199	0·403	522·4	6·324
	138·863	295	0·446	578·2	7·189
	138·760	473	0·488	632·6	8·159
157·1	157·076	8·5	0·004	5·2	1·050
	157·067	42·5	0·024	55·1	1·163
	157·061	83	0·055	71·3	1·428
	157·071	114	0·088	114·1	1·870
	157·011	126	0·109	141·3	2·152
	157·024	141	0·154	199·6	2·778
	156·984	144	0·165	213·9	2·936
	157·033	146·5	0·174	225·6	3·073
	157·115	149	0·184	238·5	3·255
	157·022	151	0·192	248·9	3·370
	157·010	154	0·203	263·2	3·570
	157·083	157	0·216	280·0	3·763
	156·966	158	0·220	285·2	3·841
	157·070	160·5	0·230	298·2	3·993
	157·109	162·5	0·238	308·5	4·085
	157·029	163·5	0·241	312·4	4·245
	157·093	163·5	0·241	312·4	4·128
	157·032	165·5	0·248	321·5	4·244
	156·991	169	0·262	339·6	4·380
	157·007	172	0·272	352·6	4·482
	157·072	174	0·278	360·4	4·494
	157·107	178	0·292	378·5	4·670
	157·045	180	0·297	385·0	4·694
	157·046	200·5	0·331	429·1	5·136
	157·113	300	0·408	528·9	6·383
	157·025	468	0·458	593·8	7·441
176·9	176·912	2·0	0·001	1·3	1·105
	176·948	2·0	0·001	1·3	1·105
	176·935	8·5	0·004	5·2	1·110
	176·801	8·5	0·004	5·2	1·097
	176·892	8·5	0·004	5·2	1·020
	176·993	9·0	0·004	5·2	1·122
	176·901	9·0	0·004	5·2	1·124
	176·916	18	0·009	11·7	1·150
	176·937	32	0·016	20·7	1·198
	176·934	43	0·022	28·5	1·220
	176·751	79·5	0·046	59·6	1·404
	176·937	102·5	0·064	83·0	1·571
	176·957	125	0·084	108·9	1·843
	176·954	156	0·130	168·5	2·399
	176·749	180	0·184	238·5	3·030
	176·805	200	0·230	298·2	3·680
	176·946	295	0·352	456·3	5·206
	176·797	475	0·427	553·6	6·649

thermal conductivity which were determined over a range of pressures at eight temperature levels. Five of the eight isotherms cover the complete pressure range from near-atmospheric pressure to 500 atm. The temperature range was 20·5° to 176·9°C, which, with the pressure range up to 500 atm, includes the gaseous and liquid phases and the critical point which is defined by $t_c = 132{\cdot}4$°C and $p_c = 111{\cdot}5$ atm [18]. For all results in the liquid-like fluid region, the corresponding density values, obtained from Davies [18], have been included in Table 1. These densities were used for a general correlation of thermal conductivity in terms of density, Section 4.3, and also for the presentation of figures in the critical region (Section 5.4). Values of density were expressed in conventional c.g.s. units (g/cm³), and in Amagat units, i.e. in terms of multiples of the density of the gas phase at 0°C and 760 mm Hg. For ammonia, one Amagat unit is equivalent to $7{\cdot}71 \times 10^{-4}$ g/cm³.

4.2 *Smoothed pressure/temperature/thermal conductivity values (Figs. 5 and 6)*

With the experimental results of Table 1, an auxiliary diagram was constructed showing the thermal conductivity as a function of pressure, with temperature as the independent parameter. From this diagram, which is not shown in this paper, values of the thermal conductivity were taken from all isotherms at selected pressures to permit the construction of a series of isobars of the thermal conductivity (Fig. 5). The selected pressures were 1 atm, and then increasing in steps

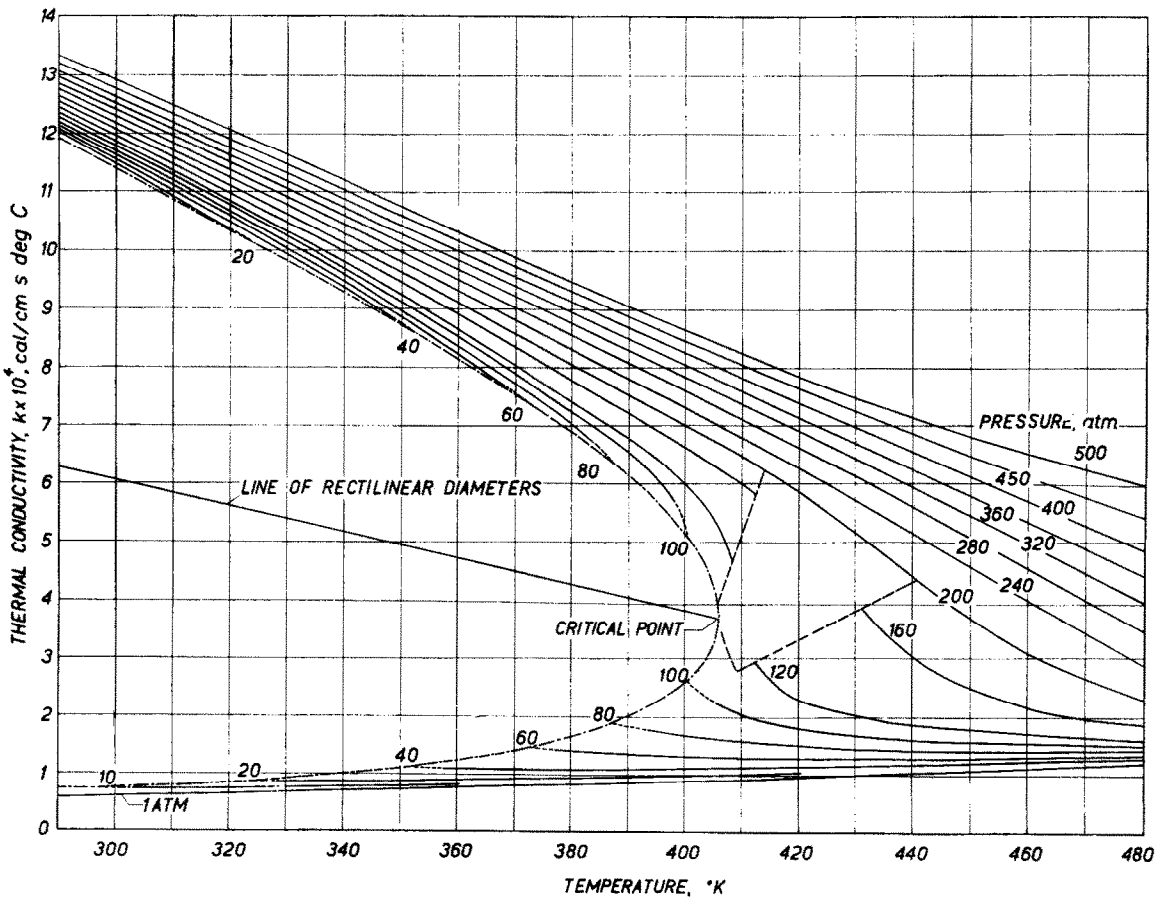

FIG. 5. Thermal conductivity of ammonia. Smoothed isobars.

of 5, 10, 20 or 50 atm to 500 atm. In conformity with a compilation of the thermodynamic properties of ammonia, frequently referred to in this paper [18], the absolute temperature scale was preferred for this and all subsequent tabulations and diagrams. To complete the graphical presentation, the isobars were extended to the appropriate saturation temperatures [18] and the liquidus and vaporus boundary curves were constructed (shown as chain-link lines in Fig. 5). To smooth the data on the boundary curves, use was made of the concept of the "rectilinear diameter" which, as orginally shown by Mathias and Kamerlingh Onnes [19], correlated the densities of the corresponding liquid and vapour phases with temperature at saturation conditions.

Extending the validity of this concept to transport properties, the arithmetic mean values of corresponding pairs of liquid and vapour thermal conductivities should lie on a straight line, the rectilinear diameter, passing through the critical point. From several corresponding pairs of results, the following equation was derived by least-square analysis for the rectilinear diameter of the thermal conductivity of ammonia.

$$10^4 \times D_k = 12{\cdot}74 - 0{\cdot}0223T \text{ cal/cm s degC}$$

where D_k is the arithmetic mean of the thermal conductivities of the liquid and vapour phases, and T the absolute temperature. Inserting the value of the critical temperature ($T_c = 405{\cdot}6°\text{K}$) in the above equation yields a value of

$$k_c = 3{\cdot}70 \times 10^{-4} \text{ cal/cm s degC}$$

for the apparent critical thermal conductivity

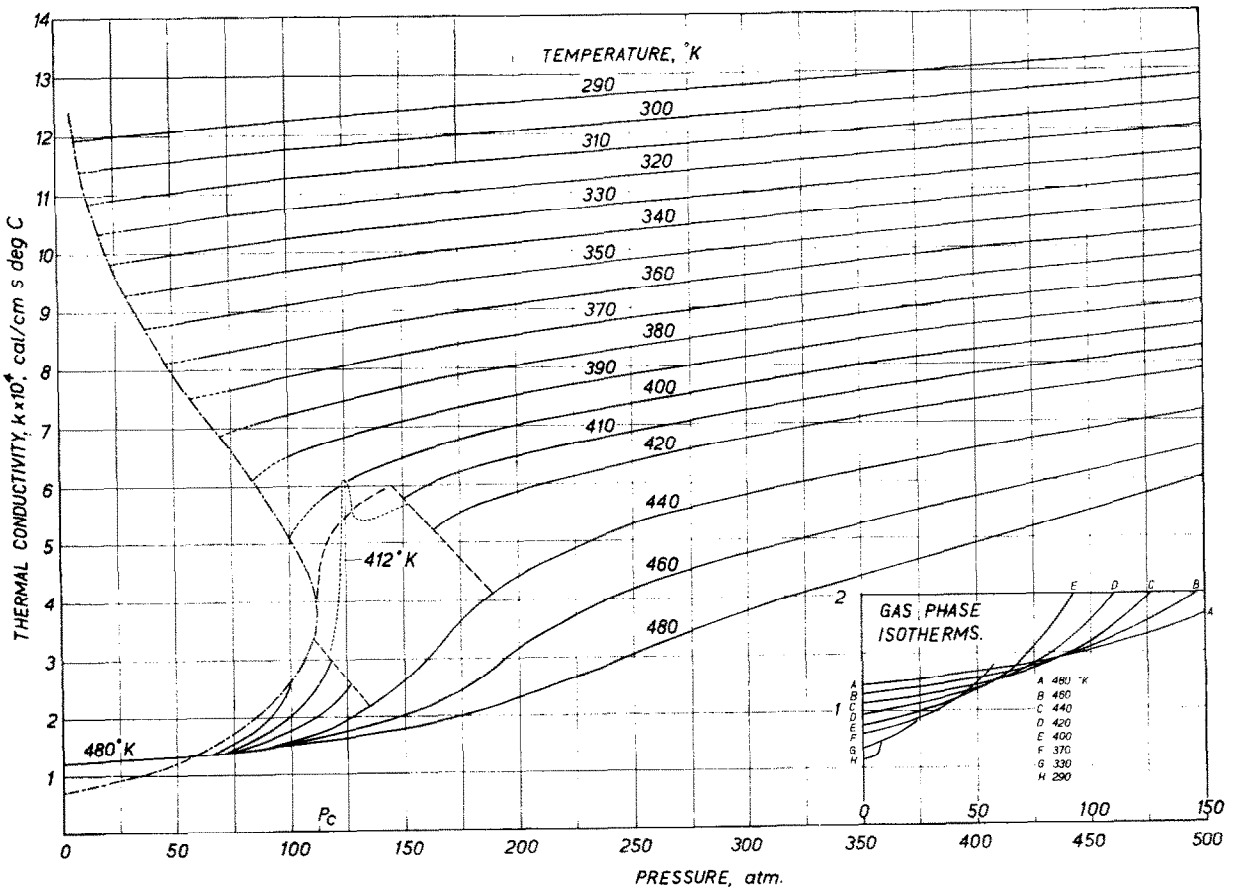

FIG. 6. Thermal conductivity of ammonia. Smoothed isotherms.

which, in view of the anomalies reported in a later section, has only theoretical significance.

By extracting values from Fig. 5 at 10 or 20 degree intervals, a smoothed plot of isotherms (Fig. 6) was constructed covering the range from 290° to 480°K. For the sake of clarity, and due to the small effect of temperature on thermal conductivity in the vapour phase, selected isotherms only are shown for the subcritical region in Fig. 6 and its inset.

It will be noted in both diagrams, that a small area near the critical point has been left blank. The smoothed isobars or isotherms terminate at the limits of this area inside which thermal conductivity has been found or is suspected to display anomalous trends which cannot be predicted by interpolation from the experimental evidence available.

To demonstrate the nature of this anomolous behaviour, a section of the 412°K experimental isotherm has been inserted in Fig. 6 and is shown by a dotted line. A detailed discussion of this phenomenon will be found in Section 5.4.

The complete range of pressure/temperature/thermal conductivity values (p—t—k) from Figs. 5 and 6 are compiled in Table 2. The intervals of pressure and temperature in this tabulation were chosen to coincide with those used by Davies [18] for the p—v—t data of ammonia, and hence direct comparison between thermodynamic properties and the thermal conductivity may be made.

The experimentally verified data to 500 atm were extended in Table 2 to 1000 atm by means of equation (2), using the density data from Davies. It is believed that the precision of these computed data is little less than that of the experimental values, and probably better than 2 per cent.

4.3 *Thermal conductivity–density correlation*

Previous investigations on the thermal conductivity of oxygen, nitrogen and argon showed the existence of a unique relation between the thermal conductivity and the density of these gases in their liquid and liquid-like fluid states [20]. To investigate whether a similar dependence obtains also for polyatomic molecules, such as ammonia, a least-square analysis was applied to 46 experimental values of the thermal conductivity and the corresponding densities, for densities exceeding the value of 0·39 g/cm³. The analysis was carried out on an electronic computer at the Royal Aircraft Establishment, Farnborough, using polynomial equations up to degree 6. The maximum deviations showed that there was no justification in considering an equation of higher than second order, and the following empirical relation appears adequate and commensurate with the accuracy of both the available density data and the thermal conductivity values of this research.

$$k \times 10^4 = 8{\cdot}695 - 27{\cdot}015\ \rho + 52{\cdot}591\ \rho^2 \text{ cal/cm s degC} \quad (2)$$

where ρ is the density in g/cm³.

In Fig. 7, the experimental values for seven isotherms are compared with equation (2).

With the exception of five points, the equation fitted the experimental results to within ±2 per cent, the largest deviation of one point being 3·2 per cent. The accuracy of the density data taken from reference 18 is not known, but, by considering the average error of both quantities to be about 1 per cent, it is seen that the experimental values are well represented by equation (2). The theoretical significance of this relation is discussed in Section 5.3. Extensive use was made of equation (2) in checking and smoothing the relevant values in Fig. 5 and 6, and in predicting dense phase figures outside the ranges of experimental verification.

4.4 *Thermal conductivity of liquid ammonia at sub-ambient temperatures*

The use of ammonia as a refrigerant makes desirable a knowledge of its thermal properties down to its freezing point, −77·7°C (195·5°K). The limitations of the apparatus used in this research precluded measurements at sub-ambient temperatures. Data do exist, however, for the density at saturation conditions in the temperature range of interest [18, 21] and hence equation (2) may be used to extend the saturation data from 290°K to the freezing point at 195·5°K. The density and calculated thermal conductivity values are shown in Table 3.

Certain aspects of the validity of the extrapolation of equation (2) to the freezing point of ammonia are discussed in Section 5.3.

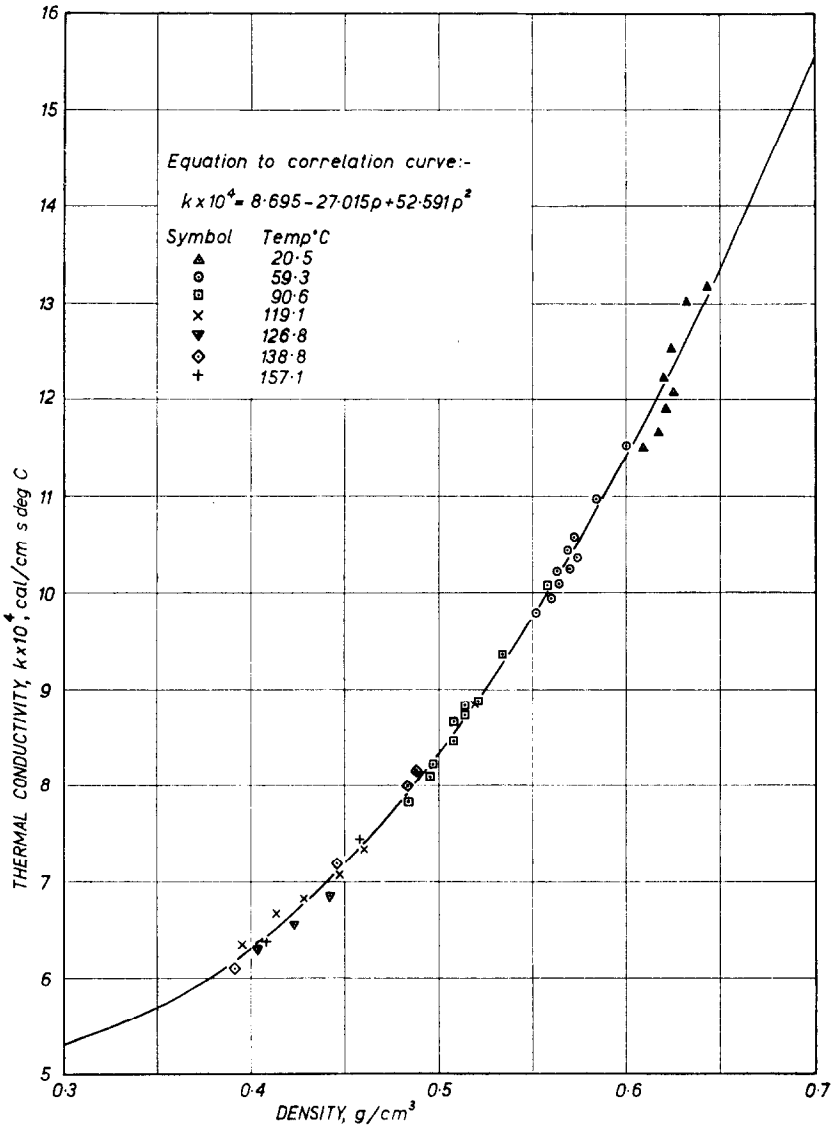

FIG. 7. Thermal conductivity of ammonia in the liquid and liquid-like fluid state versus density.

5. DISCUSSION

5.1 *Gas-phase data at 1 atmosphere pressure*

In contrast to the scarcity of information on the thermal conductivity of liquid ammonia, sufficient experimental data for the gas phase at near atmospheric pressures are available for a critical comparison with the present results [1–7].

Most observers conducted their experiments at pressures below 1 atm, whilst the lowest pressures employed in the present tests were between 1 and 4 atm. The effect of pressure on thermal conductivity within these limits is relatively small, but by no means insignificant. Hence, in order to provide a common basis for a critical analysis, all available data were reduced to 1 atm absolute pressure.

The partial derivatives of the thermal conductivity with respect to pressure, $(\partial k/\partial p)_T$, at

Table 2. Thermal conductivity of ammonia ($k \times 10^4$,

Pressure (atm)	Temperature (°K)									
	290	300	310	320	330	340	350	360	370	380
1	0·58	0·60	0·63	0·66	0·68	0·71	0·74	0·77	0·80	0·82
5	0·61	0·64	0·66	0·69	0·72	0·74	0·77	0·79	0·82	0·84
10	11·94	0·74	0·73	0·74	0·76	0·78	0·80	0·82	0·84	0·86
15	11·96	11·41	10·86	0·81	0·81	0·82	0·84	0·85	0·87	0·89
20	11·98	11·43	10·88	10·34	0·86	0·86	0·88	0·89	0·90	0·91
25	12·00	11·45	10·91	10·37	9·83	0·92	0·92	0·93	0·93	0·95
30	12·02	11·47	10·94	10·40	9·86	0·99	0·97	0·97	0·98	0·98
40	12·05	11·52	10·99	10·46	9·92	9·34	8·73	1·09	1·08	1·07
50	12·09	11·57	11·04	10·52	9·97	9·40	8·78	8·14	1·24	1·21
60	12·12	11·61	11·09	10·56	10·01	9·45	8·84	8·20	7·54	1·40
70	12·15	11·64	11·13	10·61	10·07	9·50	8·89	8·27	7·61	1·61
80	12·18	11·68	11·17	10·66	10·11	9·55	8·96	8·33	7·69	7·01
90	12·21	11·71	11·21	10·70	10·16	9·60	9·02	8·40	7·78	7·12
100	12·26	11·75	11·25	10·76	10·22	9·67	9·10	8·48	7·85	7·21
120	12·33	11·82	11·33	10·83	10·32	9·77	9·20	8·61	8·01	7·40
140	12·37	11·87	11·38	10·89	10·39	9·88	9·31	8·75	8·17	7·59
160	12·42	11·93	11·45	10·95	10·45	9·98	9·42	8·88	8·31	7·76
180	12·48	11·98	11·50	11·02	10·53	10·04	9·51	8·97	8·43	7·89
200	12·53	12·05	11·57	11·09	10·61	10·12	9·60	9·06	8·54	8·02
220	12·58	12·11	11·64	11·16	10·69	10·21	9·70	9·17	8·66	8·15
240	12·63	12·16	11·69	11·22	10·76	10·28	9·78	9·28	8·77	8·27
260	12·68	12·21	11·75	11·29	10·83	10·36	9·86	9·37	8·87	8·38
280	12·74	12·27	11·82	11·36	10·89	10·44	9·95	9·46	8·97	8·49
300	12·79	12·34	11·88	11·42	10·96	10·51	10·03	9·55	9·07	8·60
320	12·84	12·39	11·94	11·48	11·03	10·59	10·12	9·64	9·16	8·72
340	12·89	12·44	12·00	11·54	11·10	10·66	10·18	9·73	9·26	8·82
360	12·95	12·50	12·05	11·60	11·15	10·72	10·26	9·81	9·36	8·91
380	13·00	12·56	12·11	11·66	11·22	10·79	10·34	9·89	9·44	9·00
400	13·05	12·61	12·17	11·73	11·30	10·85	10·41	9·98	9·53	9·09
450	13·18	12·75	12·31	11·88	11·45	11·01	10·58	10·13	9·69	9·26
500	13·32	12·89	12·46	12·04	11·61	11·17	10·73	10·29	9·86	9·44
550	13·48	13·07	12·58	12·12	11·73	11·37	10·88	10·46	10·08	9·62
600	13·60	13·19	12·76	12·30	11·91	11·47	11·03	10·62	10·18	9·80
650	13·73	13·31	12·86	12·45	12·06	11·62	11·19	10·78	10·39	9·95
700	13·86	13·43	13·04	12·68	12·24	11·78	11·37	10·88	10·46	10·13
750	13·94	13·56	13·15	12·76	12·30	11·91	11·47	11·08	10·67	10·34
800	14·07	13·66	13·28	12·86	12·45	12·06	11·62	11·26	10·83	10·44
850	14·20	13·77	13·33	12·97	12·58	12·24	11·78	11·42	10·93	10·57
900	14·29	13·86	13·43	13·15	12·76	12·40	11·91	11·57	11·08	10·78
1000	14·46	14·03	13·69	13·33	12·97	12·58	12·24	11·78	11·42	11·03

Values above the solid lines refer to the co-existing gas phase; those below the dotted

cal/cm s degC)

390	400	410	420	440	460	480
0·85	0·88	0·92	0·97	1·06	1·14	1·22
0·87	0·90	0·94	0·98	1·07	1·15	1·23
0·89	0·92	0·96	1·00	1·09	1·17	1·24
0·91	0·94	0·98	1·02	1·10	1·18	1·25
0·94	0·97	1·00	1·04	1·11	1·19	1·26
0·97	0·99	1·02	1·06	1·13	1·20	1·27
1·00	1·02	1·05	1·08	1·14	1·22	1·28
1·08	1·09	1·11	1·13	1·18	1·25	1·31
1·20	1·18	1·18	1·19	1·22	1·28	1·33
1·34	1·29	1·28	1·27	1·26	1·30	1·36
1·52	1·45	1·39	1·35	1·33	1·36	1·40
1·83	1·68	1·56	1·47	1·41	1·42	1·44
6·29	1·98	1·75	1·61	1·50	1·48	1·48
6·52	2·62	2·03	1·78	1·59	1·55	1·52
6·75	5·96		2·28	1·87	1·72	1·61
6·98	6·31				1·92	1·74
7·18	6·60	5·98			2·17	1·87
7·36	6·82	6·27	5·59		2·58	2·05
7·51	7·00	6·47	5·85	4·38	3·12	2·31
7·66	7·16	6·65	6·08	4·80	3·60	2·59
7·78	7·29	6·79	6·26	5·12	4·00	2·89
7·89	7·42	6·95	6·45	5·40	4·30	3·20
8·01	7·55	7·09	6·62	5·60	4·54	3·49
8·13	7·68	7·23	6·76	5·76	4·76	3·76
8·26	7·81	7·36	6·90	5·94	4·96	4·00
8·37	7·93	7·48	7·03	6·10	5·16	4·23
8·48	8·04	7·58	7·14	6·25	5·35	4·45
8·57	8·13	7·69	7·26	6·38	5·52	4·67
8·66	8·23	7·81	7·38	6·53	5·69	4·88
8·84	8·43	8·03	7·63	6·84	6·11	5·45
9·02	8·61	8·22	7·85	7·14	6·54	6·00
9·21	8·80	8·44	8·10	7·42	6·84	6·29
9·33	8·95	8·62	8·18	7·67	7·07	6·53
9·56	9·16	8·81	8·46	7·85	7·26	6·73
9·69	9·33	9·04	8·67	8·05	7·48	6·96
9·90	9·51	9·18	8·82	8·23	7·70	7·14
10·08	9·67	9·32	8·95	8·39	7·84	7·29
10·18	9·85	9·50	9·16	8·54	8·01	7·48
10·39	9·98	9·78	9·31	9·69	8·18	7·67
10·62	10·34	9·96	9·62	9·95	8·46	7·96

line were computed with the aid of equation (2).

[*facing p.* 1402]

Table 3

Temperature (°K)	Density (g/cm³)	Thermal conductivity ($k \times 10^4$, cal/cm s degC)
195·5	0·734	17·20
200	0·729	16·95
210	0·717	16·36
220	0·706	15·84
230	0·696	15·37
240	0·682	14·73
250	0·669	14·16
260	0·656	13·61
270	0·643	13·07
280	0·629	12·51
290	0·615	11·97

1 atm and at various temperatures were obtained from this study by analysing a plot of the individual experimental isotherms of the thermal conductivity versus total pressure. The resultant $(\partial k/\partial p)_T$ values were plotted against temperature and were correlated by a well-fitting straight line.

With the aid of these derivatives, and assuming invariancy of $(\partial k/\partial p)_T$ over the comparatively narrow pressure interval covered by the analysis (0·25–3 atm), the results of previous observers and those of this research were reduced to 1 atm. The appropriate correction amounted to reductions of less than 2 per cent to the relevant results of this work, and increases of up to 1·7 per cent to some of the data of earlier workers.

A plot of the reduced data is shown in Fig. 8. Excellent agreement is seen to exist between all experimental results in the range from 0° to 140°C, the maximum discrepancies being about 3 per cent, but larger deviations between the data of different observers will be noticed at higher temperatures.

Until recently, no attempt had been made to apply rigorously the theory for transport phenomena of molecules with internal degrees of freedom to calculating the transport properties of strongly polar gases. Such molecules are considered to possess a hypothetical dipole located at their centres. In a theory involving molecular interactions, the additional forces due to the existence of the dipole must be considered. These dipole forces depend, apart from the field strength of the dipole itself, on the relative orientation of the two colliding molecules.

Owing to the complexity of an exact solution involving the integration of exponential functions with orientation-dependent variables, exact numerical evaluation is not available yet. However, for the special case in which the polar molecules are perfectly aligned, i.e. assuming that the dipoles are in an attractive, end-on position, the orientation factor assumes a constant value.

For this special case, Krieger [23] has calculated the collision integral, and also determined for several polar gases, from existing low-temperature viscosity data, the following molecular constants: the maximum energy of attraction ϵ, the low-velocity collision diameter

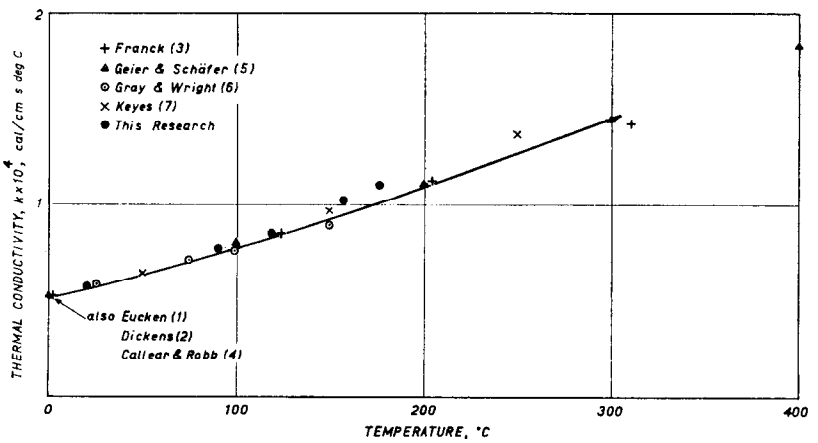

FIG. 8. Thermal conductivity of gaseous ammonia at 1 atm. A comparison of experimental data with a proposed theoretical equation of Mason and Monchick [31].

σ, and the reduced dipole parameter δ. The relevant data for ammonia were:

dipole moment $\mu = 1{\cdot}437$ debyes
$\epsilon/k = 146{\cdot}8$°K (k = Boltzmann constant)
$\delta = 1{\cdot}2499$
$\sigma = 3{\cdot}441$ Å

The thermal conductivity of a polar gas with internal degrees of freedom and the simplified molecular arrangement discussed above is given by:

$$10^5 \times k = \left(\frac{4}{15} \times \frac{C_v}{R} + \frac{3}{5}\right) \times 19{\cdot}891 \times (T/M)^{\frac{1}{2}}/(\sigma^2 . \Omega^{(2,2)}_{[T_N]}{}^*) \quad (3)$$

where

$$\left(\frac{4}{15} \times \frac{C_v}{R} + \frac{3}{5}\right)$$

is the Eucken correction,

C_v, the specific heat at constant volume, cal/degC mole,
R, the gas constant, cal/degC mole,
T, the absolute temperature,
M, the molecular weight,
and $\Omega^{(2,2)}_{[T_N]}{}^*$, the collision integral.

Using the tabulated values of the collision integral from [22] and the above fundamental molecular constants, values of the thermal conductivity computed with equation 3 were persistently higher than the experimental ones.

More recently, Mason and Monchick [31], using the formal kinetic theory of Wang Chang and Uhlenbeck [32] and of Taxman [33] derived explicit expressions for the thermal conductivity of polyatomic and polar gases by systematic inclusion of terms involving inelastic collisions and the relaxation times for the various internal degrees of freedom. Results of calculations in terms of the Eucken factor were compared with experimental results and showed a substantial improvement over the conventional and the modified Eucken coefficient, particularly as regards the temperature dependence of this quantity. To account for the anomalous behaviour of strongly polar molecules, the above authors [31] investigated the possibility of resonant exchange of energy from one molecule to another without affecting the translational energy. The results of a numerical evaluation of their relation for several polar gases, including ammonia, were presented in terms of the Eucken correction factor. Using the calculated Eucken coefficients f_{cal} and C_v values from Table 2 of [31], and values of the viscosity η of gaseous ammonia from [34], the thermal conductivity of gaseous ammonia was calculated from

$$k = f_{\text{cal}} C_v \eta / M \quad (4)$$

The calculated results are represented by the solid line in Fig. 8 which, as is seen, adequately correlates the not too numerous experimental results. Very good agreement between theory and experiment is seen to exist between 0° and 150°C. At higher temperatures greater scatter is evident and only the values of Geier and Schäfer remain in good agreement with theory. Two points of this research near 150°C are not considered very reliable because of the relatively poor thermal equilibration in the apparatus.

It seems justifiable, therefore, to tentatively propose the computed values as the most reliable values of the thermal conductivity of gaseous ammonia between 0° and 300°C at atmospheric pressure. These values, together with the other data used in this evaluation, were compiled in Table 4.

5.2 *Gas phase data at elevated pressures*

The only relevant experimental data found in literature are those of Keyes [7] who studied the thermal conductivity of gaseous ammonia between 50° and 250°C at pressures up to 9 atm. In Table 5, below, his results are in reasonable agreement with those drived from this research by interpolating in Fig. 5.

In a paper entitled "Heat conduction in highly compressed gases", Franck [12] investigated theoretically the causes for the rise in the thermal conductivity of gases at high pressures and proposed from gas kinetic considerations an approximate equation which correlates the temperature dependence of the thermal conductivity with that of the specific volume and the specific heat. This equation, which should also hold for the near critical region, is based on the following model.

Table 4

T (°K)	C_v (cal/mol degC)	$\eta \times 10^4$ (Poise)	f_{cal}	$k \times 10^4$ (cal/cm s degC)
273	6·36	0·93	1·46	0·51
373	6·99	1·26	1·51	0·78
473	7·73	1·63	1·49	1·10
573	8·48	1·98	1·47	1·45

Table 5

Pressure (atm)	Temperature (°C)	Thermal conductivity ($k \times 10^5$, cal/cm s degC)	
		Keyes	This research
5·3	50	6·74	7·02
8·5	50	6·96	7·30
4·9	150	9·85	10·00
5·4	150	10·13	10·18
5·4	250	13·84	No data
9·0	250	14·06	available

The transport of energy in gases is partly dependent upon the free movement (translation) of molecules between collisions, and partly on the transfer of energy during a collision. In a system where the mean free path becomes comparable with the effective molecular diameter, the latter mode of heat transfer will gain in importance as the energy transfer during collision is faster than the purely translational contribution. The thermal conductivity must therefore increase with increasing pressure.

The second cause, according to Franck [12], for the pressure dependence of thermal conductivity is the action of attractive forces between molecules which results in a considerable rise of specific heat with pressure in the region not too far removed from the critical point. In such a system, an additional transport of molecular interaction energy in the direction of diminishing temperature must take place and can be treated in a manner similar to the transport of chemical energy in a dissociating gas.

By relating the collisional transfer to the conductivity of the liquid at the normal boiling point, and the translational transfer to that of the rarified gas at the same temperature, the total thermal resistance of the compressed gas was thus considered as the sum of two in-series resistances represented by the reciprocals of the thermal conductivities of the liquid and gas phases weighted by the ratios of the appropriate specific volumes.

The additional energy transport by molecular interaction (clustering) was expressed by a relation similar to that derived by Eucken for dissociating gases in which the self-diffusion coefficient was chosen as the characteristic transport property.

In a comparison of his theory with available experimental data, Franck noticed serious discrepancies, and obtained better agreement by reducing the self-diffusion coefficient to half of its real value.

Based on this modified relation, Franck predicted the thermal conductivity of compressed ammonia up to 60 kg/cm^2 and 175°C. A comparison of two of his calculated isobars (20 and 60 kg/cm^2) with the present experimental values is given in Table 6 below.

At 20 kg/cm^2, the agreement between theory and experiment is satisfactory, but this can hardly be taken as proof of the theory since the pressure-induced increase of the thermal conductivity at 20 kg/cm^2 is only about 10 per cent of the value at 1 kg/cm^2.

As is seen from Table 6, the discrepancy between theory and experiment increases with rising pressure and it seems doubtful, considering the rather extensive simplifications and the necessity to introduce numerical adjustments to a physical quantity (the self-diffusion coefficient), whether the model chosen by Franck results in a better numerical prediction of the thermal conductivity of compressed gases than that predicted from the Chapman–Enskog theory of rigid spheres. The undoubted value of the above

Table 6

Temperature (°K)	Thermal conductivity ($k \times 10^4$, cal/cm s degC)			
	20 kg/cm²		60 kg/cm²	
	Franck	This research	Franck	This research
380	0·887	0·91	1·17	1·40
390	0·91	0·94	1·14	1·34
400	0·94	0·97	1·13	1·29
410	0·97	1·00	1·125	1·28
420	1·00	1·04	1·13	1·27
440	1·05	1·11	1·15	1·26

treatment lies in the fact that it has drawn attention to another phenomenon of molecular energy transport, namely that by association of molecules to clusters in regions close to the critical point. The problems and phenomena characteristic of this transitional regime will be discussed in a later section.

Another attempt to predict the transport properties of ammonia over a wide range of parameters is due to Groenier and Thodos [13] who analysed the few available data for the dense gas phase and liquid phase regions [7, 8] and treated them along the lines proposed by Abas-Zade [24]. Owing to the extreme scarcity of experimental data at higher densities, the authors found it necessary to extend the dense gas phase data by calculating the viscosity and thermal conductivity with the aid of the Chapman–Enskog theory.

With this information and the corresponding density data, reduced state diagrams for the viscosity and the thermal conductivity were constructed, extending to $T_{red.} = 10$ (4055°K) and $P_{red.} = 40$ (4460 atm), a rather ambitious undertaking, particularly when one considers that ammonia gas begins to dissociate at normal pressures at around 600°K, and that the diagram is based almost entirely on computed data.

All reduced state correlations for transport properties require the knowledge of a fictitious quantity, which can only be obtained by extrapolation, and is different from the real value, viz. the value of the transport property at the critical point itself. Recent work [25–27], confirmed by this research, has indicated that, owing to the two-phase nature of a fluid at, and immediately above, its critical point, additional energy transport phenomena come into play and appear to be responsible for the anomalous enhancement of the thermal conductivity observed in this region. These phenomena are discussed in Section 5.4.

A comparison of some dense gas-phase data, taken from the reduced state correlation of Groenier and Thodos [13], with the values from this research is found in Table 7.

Table 7

$T_{red.}$	$P_{red.}$	Thermal conductivity ($k \times 10^4$, cal/cm s degC)	
		Groenier *et al.*	This research
1·035 (420°K)	1	1·8	2·1
	2	6·1	6·1
	3	7·4	7·0
	4	8·2	7·6
	5	9·0	8·1
	6	9·5	8·5
	9	10·8	9·6
0·74 (300°K)	1	13·8	11·8
	3	14·9	12·4
	5	16·1	13·1
	9	17·3	14·0

In view of the scant experimental data that formed the basis of the work of Groenier *et al.*, and the somewhat different critical thermal conductivity value derived from the present research, it is not surprising that the agreement is not particularly good.

The undoubted value of reduced state correlations consists in making possible the prediction of data over wide ranges of parameters with a minimum of experimental effort, and with an accuracy which, for some practical applications, might well be acceptable.

Care must be taken, however, not to extrapolate such relations to conditions of state where, through the occurrence of physico-chemical changes (dissociation), and additional transport phenomena (molecular clustering), predicted values must differ seriously from the real ones.

5.3 *Liquid and solid phases*

The earliest determination of the thermal conductivity of liquid ammonia appears to be due to Kardos [8] who investigated this and other industrial refrigerants in a hot-wire cell. Experimental difficulties, believed to be caused by the electrical conductance of ammonia, prevented precise measurements and the author quoted only an average value of 12×10^{-4} cal/cm s degC derived from 25 individual measurements between $-10°$ and $+20°$C. This value is in fair agreement with the corresponding value of $12{\cdot}6 \times 10^{-4}$ computed at the mean temperature of 5°C with the aid of equation (2) and the density data of Cragoe and Harper [21].

Similar difficulties to those reported by Kardos prevented Sellschopp [9] from completing his study on the thermal conductivity of ammonia, for which he employed a horizontal, co-axial cylinder apparatus. Nevertheless, he was able to correlate his tentative results between 30° and 100°C at approximately saturation pressure by the following linear quation:

$$k = 12{\cdot}889(1 - 0{\cdot}0042t) \times 10^{-4} \text{ cal/cm s degC} \quad (5)$$

Table 8 below shows a comparison of values computed with Sellschopp's correlation equation with values derived from this research.

Excellent agreement is seen to exist between these two sets of values except at the highest temperature where the smaller value from this research indicates a more rapid decrease in the thermal conductivity as the critical point is approached. It is obvious from the shape of the boundary curves in Fig. 5 that a linear equation for predicting the thermal conductivity at saturation conditions can only hold over a comparatively narrow temperature range, and it must fail in the region close to the critical point where the boundary curve begins to display a marked curvature.

Table 8

Temperature (°C)	Thermal conductivity ($k \times 10^4$, cal/cm s degC)	
	Sellschopp	This research
20	11·80	11·74
40	10·72	10·71
60	9·64	9·64
80	8·56	8·52
100	7·47	7·31

The apparatus used in this research did not permit the determination of the thermal conductivity of solid ammonia, although such measurements are highly desirable for a better understanding of the mechanism of energy transport in the liquid phase. To the best of the authors' knowledge, only one value of the thermal conductivity of solid ammonia has ever been reported in the literature. Employing a non-steady state technique, Eucken and Englert [11] found a value of $23{\cdot}9 \times 10^{-4}$ cal/cm s degC at $-103{\cdot}9$°C. It appeared interesting to investigate whether this result can be related quantitatively to the liquid-phase values of this research. Such an analysis can serve two purposes. Firstly, it can be employed for a mere qualitative check on the validity of the proposed relation between density and the thermal conductivity of the liquid phase in the low temperature region, for which no experimental data are yet available. It is a well established fact that the thermal conductivity of a substance at the fusion point is higher for the solid than for the liquid phase. This fundamental requirement should be fulfilled therefore, by equation (2) if it is to be recommended for use in the sub-zero temperature range.

Secondly, a comparison of the solid-phase and liquid-phase thermal conductivity at the fusion point would provide an excellent opportunity of verifying current conceptions on the transport of energy in liquids, and on the structural relation between the solid and liquid states. Fusion is

accompanied by a relatively small increase of volume—in the case of ammonia about 11 per cent—and this fact alone seems to show that the arrangement of molecules in a liquid near the fusion point, must be more or less similar to their arrangement in the corresponding solid state. It must further be borne in mind that the latent heat of fusion is much smaller than the latent heat of vaporization, which implies that the cohesive forces between the molecules increase only comparatively slightly during solidification. Finally, the specific heat of condensed substances is only moderately affected by fusion, usually being somewhat higher just above the fusion point than immediately below it, except for liquids which display a strong tendency to molecular association.

All these facts seem to indicate that the mechanism of the transport of heat in liquids near their fusion points remains fundamentally the same as in solids, and is characterized by small vibrations about certain equilibrium positions, and, in the case of diatomic and polyatomic molecules, by additional rotational vibrations about equilibrium orientations. One could therefore expect that a relation capable of predicting the thermal conductivity of a liquid near its fusion point should also hold with good approximation for the immediately adjacent solid state.

To test these conceptions on ammonia, one requires ideally the values of the thermal conductivity of the liquid and solid states at the fusion point (−77·7°C). However, neither value has been determined experimentally so it was necessary to extrapolate available data to the normal fusion point as the common reference temperature.

For the solid state, use was made of a general relation for the thermal conductivity of non-metallic, polycrystalline solids, according to which the product of the thermal conductivity and the absolute temperature is constant. Using the previously mentioned result of Eucken *et al.*, the thermal conductivity of solid ammonia at the melting point was calculated as

$$k_{\text{solid}} = 20{\cdot}7 \times 10^{-4} \text{ cal/cm s degC}$$

The thermal conductivity of the liquid phase at the freezing point can be predicted with the aid of equation (2). Using a density value of 0·734 g/cm³, which was obtained by extrapolating slightly the results of Cragoe and Harper [21] to −77·7°C, a value of

$$k_{\text{liquid}} = 17{\cdot}20 \times 10^{-4} \text{ cal/cm s degC}$$

was found. Thus the first of the two basic requirements, viz. $k_{\text{solid}} > k_{\text{liquid}}$, is fulfilled.

Comparing these two values, the thermal conductivity on solidification rises by about 20 per cent, which is almost equal to the square of the corresponding density ratios,

$$(0{\cdot}81/0{\cdot}734)^2 = 1{\cdot}22.$$

In other words, the quadratic relation between the density and the thermal conductivity appears to hold also for the solid state near its transition point. Introducing into equation (2) the value of 0·81 g/cm³ from reference 28 as the corresponding density of the solid phase, yields a value of $21{\cdot}32 \times 10^{-4}$ cal/cm s degC for the thermal conductivity of solid ammonia which is only 3 per cent higher than that obtained by reducing Eucken's experimental value to the temperature of the fusion point.

From this very satisfactory agreement it was concluded that equation (2) is suitable for predicting the thermal conductivity of liquid ammonia between room temperature and the normal freezing point, and it seems probable, as postulated earlier, that there exists a strong similarity in the transport mechanism for heat in the solid and liquid states near the fusion point.

This observation will undoubtedly affect the choice of model in a general theory of thermal conductivity of the liquid state and it appears more rational to consider a liquid as a disordered solid, than to treat it as a highly compressed gas in which the free volume for translational motion is much restricted due to the close packing of the molecules.

The reference to the close agreement between an experimental and a computed value of the thermal conductivity of solid ammonia does not imply that the use of equation (2) is recommended for the solid phase beyond the freezing point. It is well understood that the thermal transport through crystalline solids follows different laws,

as is implicitly shown by the use of Eucken's relation $k_{solid} \times T = \text{constant}$.

5.4 *The critical regime*

In the preceding paragraphs of Section 5, attention has been drawn to the monotonous change of the transport properties on passing from the liquid-like to the gas-like state at supercritical pressures. However, the critical point itself and its immediate vicinity were deliberately excluded from those otherwise generally valid observations. A closer study of the properties of fluids in the comparatively narrow regime immediately above the critical point quite clearly shows unusual and interesting trends intimately connected with the changes of molecular structure characteristic of this state.

Experimental studies of the thermal conductivity near the critical point are, because of the considerable experimental difficulties, extremely scarce. Anomalous increases of the thermal conductivity of carbon dioxide at slightly supercritical conditions seem to have been reported first by Kardos [8] whose observations were later critically examined by Sellschopp [29], and were shown to have been affected by severe convection currents in Kardos' apparatus. Little importance was attached, therefore, to Kardos' attempted qualitative explanation of the nature of heat conduction near the critical point, and the problem rested for nearly 30 years.

The increasing demand in many areas of modern technology for accurate data on transport properties of fluids has led to a revival of interest in this field in recent years. Several studies of thermal conductivity of fluids have been made over ranges of temperature and pressure which included the respective critical points [20], but experimental difficulties again prevented a detailed and thorough examination of the conditions in close proximity to the critical point.

More recently Guildner [27] and Sengers [25, 26] have dealt specifically with the problem of heat conduction in the critical region. Both authors made their observations on carbon dioxide and found that the conductivity of slightly supercritical carbon dioxide is considerably enhanced, although they disagreed to some extent on the numerical values of this enhancement.

Guildner, who conducted his experiments on carbon dioxide with a vertical, co-axial cylinder apparatus, found marked increases of the thermal conductivity in the density range near the critical value of 0·478 g/cm^3 as the critical temperature is approached from higher temperatures. The isotherms of thermal conductivity versus density showed a steep maximum at the value of the critical density, and fell symmetrically towards lower and higher densities. Some additional increase was observed on the low density side at increasing temperatures. Quantitatively, the enhancement of the thermal conductivity near the critical density value at slightly supercritical temperatures was considerable, and for the isotherm 32·054°C ($T_{red.} = 1{\cdot}003$), amounted to about four times the normal value. The occurrence of the phenomenon was confined to a narrow temperature range; the enhancement of k fell sharply with rising temperature and had already disappeared at a temperature of between 40°C ($T_{red.} = 1{\cdot}029$) and 75°C ($T_{red.} = 1{\cdot}144$).

Whilst the observations of Guildner were qualitatively undoubtedly correct, justifiable doubts could be expressed concerning the accuracy of his values. Convection could not be prevented in the apparatus at conditions close to the critical point and convection-free values were determined, therefore, by extrapolating experimental results of apparent thermal conductivity to zero temperature difference. It is obvious from Fig. 4 of reference 27 that the extreme values of k near the critical density must depend very sensitively on the accuracy of the adjacent experimental points.

Further, a vertical cylinder cell is not the ideal configuration for measurements close to the critical point. Owing to the rapid change of density with pressure near this point, even pressure differences as small as the hydrostatic pressure difference between the top and the bottom of the cell result in considerable density gradients along the annulus, which, in turn, directly affect the thermal conductivity. As the heat dissipation Q is averaged over the entire surface of the cell, whilst point measurements were taken for Δt at the centre of the cell, it

follows that the thermal conductivity cannot be evaluated accurately from these two measured quantities.

These difficulties were almost completely obviated in the apparatus used by Sengers [26] in his study of the thermal conductivity of carbon dioxide at elevated gas densities. He used a flat plate apparatus with plate separation of only 0·04 cm and operated, when conditions required it, with temperature differences as small as 0·006 degC. By such drastic reduction of the vertical height of the liquid column, density gradients in the fluid can be neglected in almost all cases. The work of Sengers seems to have been carried out with great care, and as the disagreement between the work of Guildner and of Sengers is solely quantitative, and restricted to a narrow range of pressure and density where, for the reasons stated above, accurate results are almost impossible to obtain with a vertical cylinder apparatus, their main observation, i.e. that of the anomalously enhanced thermal conductivity, can be taken as established.

Neither of the two authors, however, has attempted to analyse and explain in detail the process responsible for this phenomenon. Only Sengers makes a brief reference to the behaviour of the thermal conductivity in the critical region as resembling that of the specific heat at constant volume C_v, both quantities exhibiting a distinct maximum at the critical density. Cluster formation is generally accepted to be the cause of the increase in the specific heat C_v, and the similarity between the behaviour of k and C_v led him to suggest a similar fundamental process for the enhancement of k.

The ranges of pressure and temperature of this investigation include the critical point of ammonia and it appeared important to take the opportunity to confirm the observations of those authors on another substance.

The measurements that were carried out in the region of the critical density along the two supercritical isotherms at 139° and 157°C ($T_{\text{red.}} = 1{\cdot}016$ and 1·061, respectively) have been mentioned in earlier sections of this paper (3.5.6 and 3.7.2), where details of the experimental technique can be found. Figure 9 shows that whilst the deviation from "normal" behaviour was only moderate along the 157°C isotherm, a considerable rise of the thermal conductivity was observed at 139°C in the density range 200 to 400 Amagat, with a maximum near 250 Amagat which is somewhat below the reported critical density of 305 Amagat. It will be noticed further that the two isotherms converge towards each other outside the above mentioned density range. They can be represented by a single line above 500 Amagat, and show little difference from each other below 150 Amagat. The experimental isotherm 177°C ($T_{\text{red.}} = 1{\cdot}110$) shown in the same diagram represents a characteristic example of the so-called "normal" behaviour. By "normal" behaviour, it is understood that the thermal conductivity k monotonously increases with the density ρ, and that neither maxima or minima of k, nor inversion points, may exist for the functional relation k and ρ. This condition finds its analytical expression in

$$\partial k/\partial \rho \neq 0 \quad \text{and} \quad \partial^2 k/\partial \rho^2 \neq 0$$

Taking the 177°C isotherm as a datum line, the vertical displacements of the other two isotherms from this line in Fig. 9 can be taken as the contributions Δk of an additive transport phenomenon; these are represented by the two dotted lines in Fig. 9. It will be noticed that each of the two curves, of Δk vs. density, possesses a maximum at a distinctly different density, viz. at 250 Amagat for the 412°K isotherm, and at 314 Amagat for the 430·3°K isotherm. The pressures corresponding to these conditions of state were found by graphical interpolation of the data in reference 18 as 125 and 164 atm respectively.

A cursory examination of the location of the maximum of k indicated a close proximity to the maximum of the specific heat at constant pressure C_p, but the exact location of the maximum of C_p in terms of p and T cannot be obtained for ammonia with sufficient accuracy from either the tables or the diagrams in reference 18.

The relationship between the temperature of a given maximum of C_p and the pressure has been discussed by Jones and Walker [30], who, from their measurements of the specific heats of argon, concluded that these maxima can be located with fair precision, and that the values of pressure and temperature corresponding to the maxima

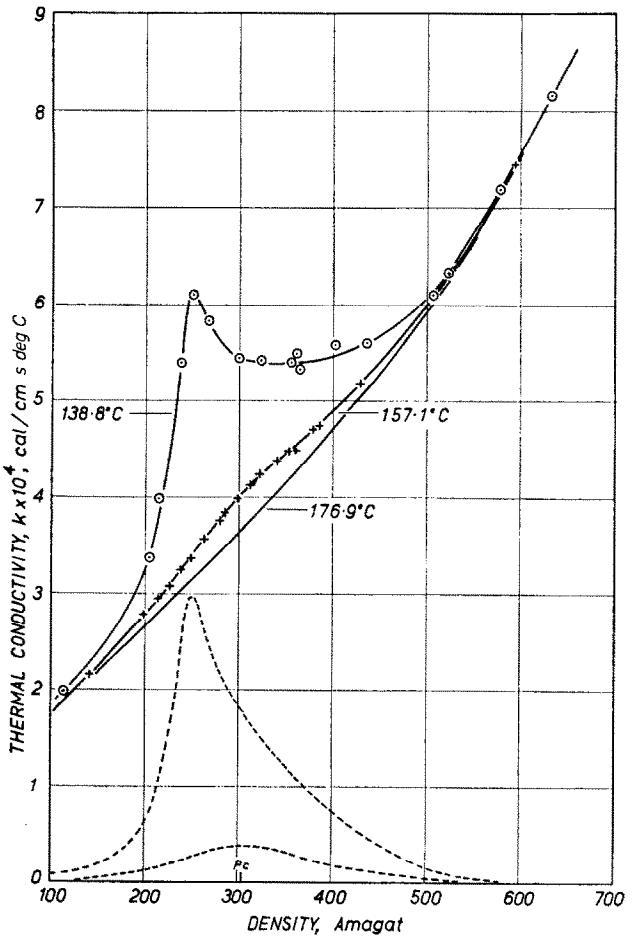

FIG. 9. Anomalous enhancement of the thermal conductivity in the critical region.

of C_p $(\partial C_p/\partial_p)_T = 0$ lie exactly on the extrapolated vapour pressure curve in the p–T diagram. The significant feature of this result is that it illustrates how sharply even the extrapolated vapour pressure curve divides the fluid region of the field into liquid-like and gas-like regions.

It seemed justifiable to assume that this observation has general validity and applies equally well to ammonia. Examination of the existing saturation data for ammonia showed that they can be correlated by a linear equation between log p and $1/T$ (Fig. 10). To check the validity of the above postulate, the line was extended beyond the critical point and approximate values of p and T for $C_{p\,\max.}$ were derived from an analysis of the C_p/T diagram of reference 18. As is seen, the individual points are indeed closely grouped on either side of the extended saturation curve.

With the aid of Fig. 10, the corresponding pressures for the maxima of C_p at 412° and at 430°K were found to be 123 and 166 atm respectively. These values are in close agreement with those found for the corresponding pressures of the maxima of Δk, which were 125 and 164 atm respectively.

This research has confirmed the occurrence of maxima of the thermal conductivity at slightly supercritical temperatures as reported by previous observers [8, 25–27] who also showed that

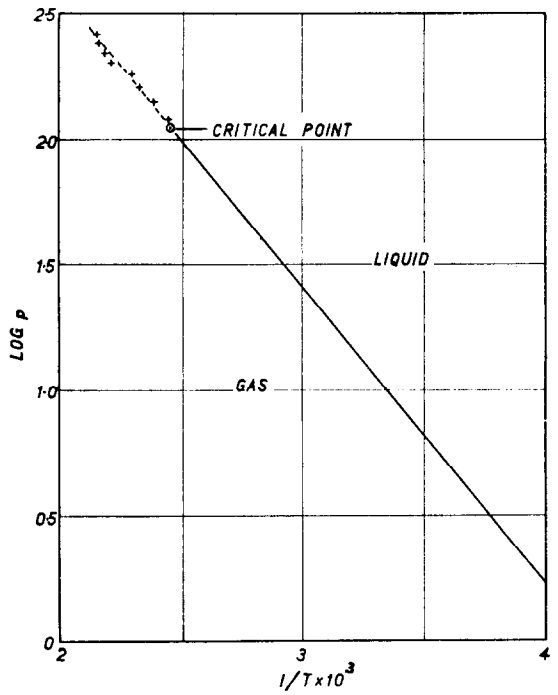

FIG. 10. Saturation vapour pressure of ammonia as a function of the temperature, showing the location of the maxima of the specific heat C_p along the extension of this line.

the location of these maxima coincided with that of the corresponding maxima of the specific heats, C_p or C_v. This is borne out by the maximum of k for the 157·1°C isotherm of this research, but the maximum of the isotherm at 138·8°C occurs at a density less than the critical value.

As that value of density was obtained by graphical interpolation, the possibility of an error in the density cannot be ruled out, and no positive conclusion should be drawn, therefore, from this apparent discrepancy on the location of these extreme values.

The results of further studies, preferable on some additional substances, are essential for further theoretical treatment of this phenomenon.

ACKNOWLEDGEMENT

Crown Copyright reserved. Reproduced by permission of the Controller, H.M. Stationery Office.

REFERENCES

1. A. EUCKEN, *Phys. Z.* **14**, 324 (1913).
2. B. G. DICKENS, *Proc. R. Soc.* **A143**, 517 (1934).
3. E. U. FRANCK, *Z. Elektrochem.* **55**, 636 (1951).
4. A. B. CALLEAR and J. C. ROBB, *Trans. Faraday Soc.* **51**, 630 (1955).
5. H. GEIER and K. SCHÄFER, *Allg. Wärmetech.* **10**, 70 (1961).
6. P. GRAY and P. G. WRIGHT, *Proc. R. Soc.* **A263**, 161 (1961).
7. F. G. KEYES, *Trans. Am. Soc. Mech. Engrs.* **76**, 809 (1954).
8. A. KARDOS, *Z. Ges. Kälteind.* **41**, 1 (1934).
9. W. SELLSCHOPP, *Z. Ver. Dt. Ing.* **75**, 69 (1935).
10. B. H. SAGE, Private Communication (1961).
11. A. EUCKEN and H. ENGLERT, *Z. Ges. Kälteind.* **45**, 109 (1938).
12. E. U. FRANCK, *Chemie-Ingr-Tech.* **25**, 238 (1953).
13. W. S. GROENIER and G. THODOS, *J. Chem. Engng Data* **6**, 240 (1961).
14. H. ZIEBLAND and D. P. NEEDHAM, Amer. Soc. Mech. Engrs, 2nd Symposium on Thermophysical Properties (1962).
15. H. ZIEBLAND and J. T. A. BURTON, *Int. J. Heat Mass Transfer* **1**, 242 (1960).
16. E. W. COMINGS, *High Pressure Technology*, p. 71. McGraw-Hill, New York (1961).
17. L. ADDICKS, Ed., *Silver in Industry*. Reinhold, New York (1940).
18. P. DAVIES, *Ammonia in Thermodynamic Functions of Gases*, F. DIN, Ed. Butterworths, London (1956).
19. E. MATHIAS and H. KAMERLINGH ONNES, *Leiden Commun.*, No. 117 (1911).
20. H. ZIEBLAND, *Dechema Monogr.* **32**, 74 (1959).
21. C. S. CRAGOE and D. R. HARPER, *U.S. Bur. Stand. Sci. Papers* **20**, 65 (1924).
22. J. O. HIRSCHFELDER, C. F. CURTIS and R. B. BIRD, *Molecular Theory of Gases and Liquids*. John Wiley, New York (1954).
23. F. J. KRIEGER, USAF Project Rand, *RM*-646 (1951).
24. A. K. ABAS-ZADE, *Zhur. Eksp. Teor. Fiz.* **23**, 60 (1952).
25. J. V. SENGERS and A. MICHELS, Amer. Soc. Mech. Engrs, 2nd Symposium on Thermophysical Properties (1962).
26. J. V. SENGERS, Thesis, University of Amsterdam (1962).
27. L. A. GUILDNER, *J. Res. Natn. Bur. Stand., Wash.* **66A**, 333 (1962).
28. E. C. FRANKLIN, *The Nitrogen System of Compounds*, Amer. Chem. Soc. Monograph 68. Reinhold, New York (1935).
29. W. SELLSCHOPP, *Forsch. Geb. IngWes.* **5**, 162 (1934).
30. G. O. JONES and P. A. WALKER, *Proc. Phys. Soc.* **69B**, 1348 (1956).
31. E. L. MASON and L. MONCHICK, *J. Chem. Phys.* **36**, 1622–1639 (1962).
32. C. S. WANG CHANG and G. E. UHLENBECK, *Univ. Michigan Engng Res. Rep.* No. *CM*-681 (1951).
33. N. TAXMAN, *Phys. Rev.* **110**, 1235 (1958).
34. R. KIYAMA and T. MAKITA, *Rev. Phys. Chem. Japan* **22**, 49 (1952).

Résumé—La conductivité thermique du gaz ammoniac et de ce gaz liquéfié a été déterminée entre 20° et 177°C et à des pressions allant de 1 à 500 atmosphères en employant un appareil à cylindres coaxiaux verticaux.

Des mesures au voisinage du point critique (p_c = 111,5 atm, t_c = 132,4°C) ont été poursuivies avec un soin spécial le long des isothermes réduites 1,016 et 1,061. On a trouvé une augmentation anormale de la conductivité thermique dans ce régime, semblable à celle du gaz carbonique remarquée auparavant par deux autres observateurs. On a essayé de donner une explication de ce phénomène, basée sur le transport d'énergie par des groupes de molécules.

Les résultats expérimentaux pour l'état fluide presque liquide, à la fois en-dessous et au-dessus de la température critique, ont été corrélés par une équation quadratique entre la densité et la conductivité thermique. A l'aide de cette équation, on a calculé des valeurs pour les conditions en dehors de celles de cette étude, et le tableau contenant les nombres lissés et vérifiés expérimentalement pour des augmentations paires de pression et de température a été complété par des valeurs calculées allant jusqu'à 1000 atm et 480°K. Les valeurs calculées sont aussi présentées sous la forme de tableau pour la gamme de températures importante pour la technique allant de la température ambiante au point de fusion normal (195,5°K).

Pour obtenir une revue générale, et pour une interpolation rapide, les résultats expérimentaux sont présentés également sous la forme de deux diagrammes, dans lesquels sont tracés les isobares et les isothermes de la conductivité thermique, en utilisant respectivement la température et la pression comme variables indépendantes.

Les données, pour la phase gazeuse à faible pression, des expérimentateurs antérieurs et des auteurs ont été réduites à latm à l'aide des coefficients de pression obtenus à partir de cette étude. En employant la relation pour la conductvité thermique des gaz polaires, proposée par Mason et Monchick, les résultats de toutes les référence ont été corrélés d'une façon satisfaisante entre 300° et 500°K.

Les résultats de ce travail sont en bon accord avec les quelques données de la phase gazeuse dense par Keyes, et avec les données expérimentales le long d'une petite partie de la ligne de saturation donnée par Sellschopp dans la seule référence que l'on ait trouvée sur la conductivité thermique de l'ammoniaque liquide.

En considérant toutes les causes d'erreurs, on estime que la précision de cette étude est inférieure à ± 1,5% pour les phases liquide et gazeuse, dense, et inférieure à ± 2% pour la phase gazeuse à faible pression et dans la région près du point critique.

Zusammenfassung—Mit Hilfe einer Apperatur aus vertikalen, coaxialen Zylindern wurde die Wärmeleitfähigkeit von flüssigem und gasförmigen Ammoniak zwischen 20° und 177°C und bei Drücken von 1 bis 500 atm bestimmt.

In der Nähe des kritischen Punktes (p_c = 111,5 atm, t_c = 132,4°C) wurden Messungen mit besonderer Sorgfalt längs den reduzierten Isothermen, 1,016 und 1,061 durchgeführt. In diesem Bereich ergab sich ein anomaler Anstieg des Wärmeleitvermögens ähnlich dem von Kohlendioxyd, worüber vor kurzem andere Forscher berichteten. Es wird eine vorläufige Erklärung dieser Erscheinung angegeben, die auf dem Energietransport von Molekülballungen basiert.

Versuchsergebnisse für den flüssigkeitsähnlichen Zustand des Mediums sowohl unter als auch über der kritischen Temperatur wurden in einer quadratischen Gleichung zwischen Dichte und Wärmeleitfähigkeit miteinander verbunden. Mit Hilfe dieser Gleichung wurden Werte für Zustände, die von dieser Arbeit nicht erfasst werden, berechnet, und die Tabelle mit den glattesten, experimentell verifizierten Kurven für gleichen Druckund Temperaturanstieg mit berechneten Werten, die bis zu 1000 atm und 480°K reichen, ergänzt. Ebenso werden rechnerisch ermittelte Werte in Tabellenform für den für die Technik wichtigen Temperaturbereich von Zimmertemperatur bis zum normalen Fusionspunkt (195,5°K) angegeben.

Für einen allgemeinen Überblick und für die schnelle Interpolation werden die Versuchsergebnisse auch in Form von zwei Diagrammen aufgeführt, in denen die Isobaren and Isothermen der Wärmeleitfähigkeit gezeigt werden, wobei die Temperatur bzw. der Druck als unabhängige Variablen verwendet werden.

Mit Hilfe von aus dieser Arbeit abgeleiteten Druckkoeffizienten wurden früher bestimmte Daten für kleine Drucke der Gasphase und die Daten aus dieser Untersuchung auf 1 atm reduziert. Unter Verwendung der von Mason und Monchick vorgeschlagenen Beziehung für die Wärmeleitfähigkeit polarer Gase wurden die Ergebnisse aller Quellen zwischen 300° und 500°C zufriedenstellend korreliert.

Die Ergebnisse dieser Arbeit stimmen mit den wenigen, von Keyes für die dichte Gasphase angegebenen Werten gut überein und mit den vorläufigen Werten längs einer Kurvenstrecke der Sättigungslinie, die von Sellschopp in dem einzigen aufgefundenen Quellennachweis über die Wärmeleitfähigkeit von flüssigem Ammoniak angegeben werden, völlig überein.

Unter Berücksichtigung aller bekannter Fehlerursachen wird die Genauigkeit dieser Arbeit auf innerhalb ± 1,5% liegend für die flüssige und dichte Gasphase und auf innerhalb ± 2% liegend für die Gasphase bei kleinen Drücken und für den Bereich in der Nähe des kritischen Punktes geschätzt.

Аннотация—С помощью вертикального коаксиального цилиндра измерялась теплопроводность жидкого и газообразного аммиака при температурах от 20 до 177°С и давлениях от 1 до 500 атм.

Проведены измерения вблизи критической точки (P_c = 111,5 атм, t_c = 132,4°С), при чем особое внимание обращалось на изотермы 1,016 и 1,061. Обнаружено аномальное увеличение теплопроводности при этих параметрах, аналогичное ранее описанному другими авторами поведению двуокиси углерода. Приводится предположительное объяснение этого поведения, в основу которого положен перенос энергии группами молекул.

Экспериментальные данные по состоянию капельной жидкости при температуре ниже и выше критической обрабатывались с помощью квадратного уравнения, связывающего плотность с теплопроводностью. С помощью этого уравнения подсчитаны значения для условий, не исследованных в данной работе. По экспериментально определенным и подсчитаным значениям теплопроводности составлялись таблицы в пределах давления до 1000 атм и температуры до 480°К. Эти значения протабулированы в форме, удобной для технических расчетов в температурном диапазоне от комнатной температуры до нормальной точки плавления (195,5°К).

Для удобства обобщения и быстрой интерполяции, экспериментальные данные представлены также в виде двух графиков, где изобары и изотермы построены с использованием давления и температуры, соответственно, в виде независимых переменных.

Данные в газовой фазе при низком давлении других исследователей, а также результаты настоящей работы приведены к одной атмосфере с помощью коэффициентов давления, полученных в этом исследовании. Результаты всех работ удовлетворительно обобщаются в пределах от 300 до 500°К с помощью формулы теплопроводности полярных газов, предложенного Мейсоном и Мончиком.

Результаты этой работы хорошо согласуются с немногочисленными данными по плотной газовой фазе, опубликованными Кейесом, и находятся в полном соответствии с экспериментальными данными, полученными на коротком участке линии насыщения, опубликованными Селлшопом в единственной работе по теплопроводности жидкого аммиака.

С учетом всех возможных источников погрешностей, точность этой работы составляла ±1,5% для жидкой и плотной газовой фаз и ±2% для газовой фазы при низком давлении и в околокритической области.